Chapter 1

LITERATURE SURVEY

The promise of Ultra-Wideband Communication for high speed connectivity, greater data rate, lower hardware cost, and lower complexity in system are the main reason for increasing interest in the study of Ultra wide-band communication. As it is clear from the name, Ultra Wide-band means a large band of frequencies.

1.1 **Motivation**

This study deals with the problem of accurate prediction of the ultra wide-band channel. Due to huge Band-Width for a UWB signal, all the basic principles of propagation models needs to be re-examined. The propagation of UWB signals in indoor/outdoor environments is one of the key issues with significant impacts on the future direction, scope, and the extent of the success of UWB technology.

UWB communication systems employ very short duration pulses, which are usually 1 ns wide, for both transmission and reception. Therefore, UWB signals are very flexible to the multipath phenomena. Due to its limit on PSD (imposed by FCC) its PSD is very low and it is received by other communication system as noise. In the narrow band communication, the response of the channel to the noise is nearly flat, and that is why the distortion in the signal is very nominal. The shape of received signal is almost unaffected for a narrow band signal over transmission through a channel. For UWB communication, since the BW of the UWB pulse is extremely large and each multipath component is frequency dependent with its own impulse response of each multipath component. Thus, the receiver receives a distorted pulse after transmission through a channel. UWB signals employ many advantages such as: (i) Accurate position location (ii) multiple access due to wide transmission bandwidths (iii) possibility of extremely high data rates (iv) possible easier material penetration, to be named

few. For realizing such a system that is so much efficient we need to properly estimate the channel so that the distortion in the signal can be known. Furthermore in order to properly design a optimum rake receiver, the UWB pulse distortion (i.e. channel characteristics) should be known.

There are two approaches which is used in order to analyze the distortion in the UWB pulse: (i) First obtain frequency-domain (FD) solution of the propagation channel and then taking IFFT of the results obtained (ii) Direct time-domain (TD) solution. Since UWB signal has a very broad frequency range, it is very computationally inefficient to apply the former approach to determine the frequency response of the channel and so its pulse distortion. It is more convenient to work directly in time-domain. Moreover, with the help of the TD approach, the impulse response of the channel model can be calculated and it is convolved with the transmitted pulse to predict the received signals. All the detailed features which are of importance in the UWB system, such as the time delay, the power and the pulse shape/distortion can be obtained very easily with the help of TD approach. It is also helpful in determining time delay parameters of the wireless channel which is of great importance in application involving synchronization, positioning and detection.

1.2 Literature Survey

Efficient and reliable propagation model can optimize the network planning and reduce unnecessary interference. Efficient propagation model can result in proper utilization of economy of mobile industry by providing effective communication and thus increasing number of services per cell. Deterministic modeling is the most considerable solution to the modeling of wireless propagation channel. Diffraction is a dominant phenomena in propagation modeling which is always encountered from building edge, hilly terrain etc. Linear-piece wise model is being widely accepted now-a-days to model such profile. Geometrical theory of diffraction (GTD) and Uniform Theory of diffraction were widely used by researchers for the modeling of wedges. The earlier deterministic modeling of wireless channel was mainly performed by Geometrical Theory of diffraction (GTD) [5] and its extension Uniform Theory of diffraction [6]. GTD gives acceptable result in illumination region for the prediction of diffracted field but it fails to predict the diffracted field in the

shadow region. Uniform theory of diffraction is based on clemmow method of steepest descent gives an acceptable result in the shadow region too (though not accurate).

Pathak [6] formulated a UTD approach which gives a solution to the GTD formulation problem for a perfectly conducting wedge, when a electromagnetic wave is incident on it. So, this diffraction coefficient was limited for only perfectly conducting wedges. So as to make the UTD coefficient applicable to the wedge (lossy dielectric) which are not perfectly conducting, Luebbers [7] modified the result by multiplying the Fresnel Reflection coefficient to the component of diffraction coefficient. With this, the coefficient became workable for the lossy dielectric wedges. The heuristic coefficient by Luebbers gives accurate result in the vicinity of the reflection boundary but not in a deep shadow region. Kate a Ramley et al [41] improved the accuracy of Leubbers coefficient in shadow region by introducing new reflection angles for the calculation of reflection coefficient. To improve accuracy of Luebbers heuristic coefficient, Holm[8] further modified the original coefficient formulated by luebbers with a multiplication factors to be used in the coefficient. This improvement gives a very reliable result in the shadow region. However this coefficient was not able to predict diffraction field accurately in the illumination region. El Sallabi [9] proposed a modification to Holm's Coefficient which was in a good agreement to the Rigorous [15] Solution. Sallabi modified the angle definition used in the reflection coefficient and modified the Fresnel reflection coefficient too. But these coefficient were neither reciprocal nor symmetric. The rigorous solution to the imperfectly conducting wedge problem was introduced by Maliuzhinets. The main issue with the implementation of Rigorous Diffraction Coefficient (RDC) for any propagation channel was its computational complexity. It is very difficult to compute Maliuzhinets function [9] for an arbitrary wedge angle, so these solutions are not practical for path loss predictions over real terrain due to the complexity of problem.

The above diffraction coefficients were neither reciprocal nor symmetric. Aidi et al [14] proposed new angle definition for the reflection coefficient. D. N. Schettino [13] used the new angle definition proposed by Aidi et al, and defined a new reciprocal heuristic coefficient which showed clear agreement to the previously defined heuristic coefficients. However, this coefficient has a limitation that it was reciprocal only when the transmitter and

receiver were on the either side of wedge. But when the transmitter and receiver were on the same side, the diffraction coefficient was not reciprocal. S. k. Soni [16] further improved these diffraction coefficients by defining a new diffraction coefficient which was both reciprocal and symmetric and showed very good agreement with Rigorous solution.

All the above diffraction coefficients were proposed for frequency domain and as it is preferable to work directly in time-domain. Each and every parameters that can be calculated in UWB system, such as the number of multipath, the delay, the power, and the distortion of every single path are easily evaluated with the help of TD profile [25]. FD solution involves the calculation of channel response for every frequency separately, which is very inefficient for such large bandwidth as in UWB signal. It is rather feasible to work directly in time-domain than to first evaluate the response in frequency domain and then taking its inverse Fourier transform [18]. In the TD approach, a general solution from the impulse response of a resultant path is considered, irrespective of band-width and this resultant impulse response can be convolved with any transmitted signal. The TD coefficients thus can be inserted into the channel, which will thus predict the distortion in the signal.

Pathak formulated the TD coefficient for UTD case, that is called TD UTD_PO [23,24] formulations and its application to various single, double and multiple diffraction are presented in [22,25-30]. For the calculation of diffracted field and distorted pulse mainly Holms coefficient was used. In this work, time domain formulation of all the defined heuristic approach has been proposed. All these heuristic coefficients are then compared with the inverse Fourier transform of Rigorous solution [15]. Furthermore, the symmetry and reciprocity in time domain have been evaluated from these time domain heuristic coefficient formulations.

In urban microcellular scenario and indoor scenario especially in non-line of sight (NLOS) communication in deep shadow regions, where the reflected and diffracted field components are weak, transmitted field component proves to be very significant [31]. So it becomes important to analyze the effect of transmitted field through a wall for UWB communication in microcellular and indoor scenario. The TD solutions for transmission of UWB signals through a dielectric slab were presented in [12, 40]. Here multiple reflections inside the slabs were ignored due to their weak contribution. Another TD solution for transmission through a dielectric slab, considering a limited number of internal reflections, was presented in [35,36].

The measurements depicting the characterization of different materials within UWB range along with the discussion about dispersion suffered by UWB signals due to penetration through the walls were presented in [36]. According to them, in certain cases, the multiple reflections inside the slab decay rapidly. In such cases, the single pass and multiple pass techniques provide the same results. Another work in [36] presented UWB pulse reflections and transmissions through complex wall structures, found in indoor propagation environments, through numerical FDTD simulations. A simplified TD model for transmission of UWB signals through a dielectric slab was presented in [12, 40]. The TD solutions for the reflection and transmission through a dielectric slab incorporating the multiple internal reflections, was presented in [34]. In [39], a TD transmission coefficient for transmission through an interface involving free space and dielectric material has been studied and structures like single wedge and single building scenarios have been analyzed. Though a TD model for UWB signals transmitting through a dielectric slab with interface having free space and dielectric medium exists in literature [32, 33, 37]. In our work we have considered the multi-modeled obstacle, in which UWB signals transmitted through the wall of building and then it will arrive at the receiver. We have proposed TD solution for received field calculation after penetration through our considered obstacle.

1.3 Organization of Thesis

Chapter 2: The chapter deals with the overview of Ultra-wide band communication. This chapter starts with introduction to the ultra wide-band signal and its main properties and key benefits due to which it is the primary focus of the researchers. Rest of the chapter deals with the major application of the ultra wide-band signal.

Chapter 3: In this, different Time-Domain heuristic coefficients for the diffraction through wedge are considered. Three regions are considered to analyze the result in time-domain and the ray tracing is considered in this chapter.

Chapter 4: The Time-domain solution for transmission for a 2-D & 3-D multi-modeled obstacle is presented. The multi-modeled obstacle considered is a dielectric wedge followed by a dielectric slab.

Chapter 5: It analyzes the results of the simulations & results, and in this way different heuristic time domain coefficient have been studied for the different positions of transmitter and receiver and it can be seen that which coefficient gives a better result in which region. The time-domain result for transmission in a multi-modeled scenario is also compared with the IFFT of the F-D solution.

Chapter 6: In this chapter we will conclude the work and importance of our work for the accurate prediction of channel. This chapter also contains some suggestion for the future work.

Chapter 2

Overview of Ultra-Wideband Communication

UWB signals are defined as signals with either a large relative bandwidth (typically, larger than 20%), or a large absolute bandwidth (> 500 MHz) as per defined by FCC [1]. Ultra-Wideband pulse is a very narrow pulse with nominal energy. Due to such a huge bandwidth, it can be proved very much suitable for both communications and radar applications. This technology is different from conventional narrowband wireless transmission technology-instead of broadcasting on separate frequencies; UWB spreads signals across a very wide range of frequencies. The typical sinusoidal radio wave of narrow band signal is replaced by train of narrow pulses per second.

2.1 Key Benefits of UWB

2.1.1 High Data Rate

The high data rate is one of the most attractive aspects if a user's point of view or any commercial manufacturer's position is considered. New applications and devices that would not have been possible up until now can now be designed with higher data rate. Speeds of over 100 Mbps have been demonstrated, and there is still a scope for higher speeds over short distances. This much high data rate for a UWB signal can be explained by examining Shannon's famous capacity equation. Shannon's equation [2] is expressed as:

$$C = B\log\left(1+\frac{S}{N}\right)$$

Where C is the maximum channel capacity (bits/second), B is the channel Bandwidth (Hz), S is the power of the signal in watts (W) and N is the power of the noise in watts (W). As it is clearly visible from the equation that channel Capacity increases linearly with Bandwidth but

logarithmically with signal power. UWB signal have huge bandwidth, that's why despite of very less power contained in UWB signal, it has a very high data rate.

2.1.2 Multipath Immunity

UWB pulses are extremely narrow, so they can be filtered or ignored. UWB signal can readily be distinguished from unwanted multipath copies which are reaching the receiver at different times and with different distortions because of the fine time resolution. This fine time resolution leads to a very exciting feature of multipath immunity. This is important in any wireless communication, as if pulses (or sinusoids) interfere with each other can lead to the major obstacles to error-free communication. Multipath effect is caused due to the physical phenomena viz. reflection, scattering and diffraction of electromagnetic energy by objects which form the channel between the transmitter and the receiver. In UWB, narrow pulses are too short that if it is atleast separated by more than one pulse width from its reflection copies, they will not interfere.

2.1.3 Low Equipment Cost

The ability of Ultra-Wideband signal to directly modulate a pulse onto an antenna is perhaps as simple as a transmitter can be made, leading to possibilities where extremely cheap transceivers can be designed. This is possible because many of the components required for conventional sinusoidal transmitters and receivers can be eliminated. The low component count leads to remarkable reduction in cost, and smaller chip sizes lead to low complexity in systems. The simplest UWB transmitter could be assumed to be containing a pulse generator, a timing circuit, and an antenna. Expensive and large components, such as modulators, demodulators, IF stages are not required in the design of transmitter and receiver for UWB signal. All these factors lead to reduced cost, size, weight, and less power consumption of UWB systems when compared with conventional narrowband communication systems.

2.1.4 Ranging and communication system at same time

The use of both precise ranging (object location) and high speed data communication in the same wireless device presents possibilities for new devices and applications

2.2 Basic Properties of UWB Signal and Systems

2.2.1 Power Spectral Density (PSD)

The power spectral density (PSD) of UWB system is extremely low, especially for communication applications. The PSD is defined as:

$$PSD = \frac{P}{B}$$

Where P is the power transmitted in watts (W), B is the bandwidth of the signal in hertz (Hz), and so the unit of PSD can be defined as watts/hertz (W/Hz). For a UWB system the pulses have a short time duration t and very wide bandwidth B. One of the key benefits of low-PSD is a low probability of detection, which can be proven useful for military applications. This is also a concern for wireless consumer applications, where the security of data for corporations and individual is of great concern.

2.2.2 Pulse Shape

The figure 1(a) shows a typical Ultra-Wideband signal known as Gaussian doublet. It is the mostly used signal shape in ultra wideband communication because of the simplicity in the generation of this signal. This pulse can be described as simply a square pulse which is generated by limiting the rise and fall times of pulse, and filtering effect of transmit and receiving antennas. A square pulse can be shaped so by switching the transistor on and off rapidly. Ultra Wideband signal are narrow pulses of order of nanoseconds and picoseconds. This rapid switching on and off leads to a shape with smooth edges. This pulse approximates a curve with a Gaussian shape curve [19]. For UWB communication, the pulse is transmitted directly without modulation to the antenna which results in filtering of pulse due to the properties of antennas. The filtering operation is just a derivative operation. The same process of filtering take place at the receiving antenna. Figure 1(b) shows the spectrum of Ultra wideband signal.

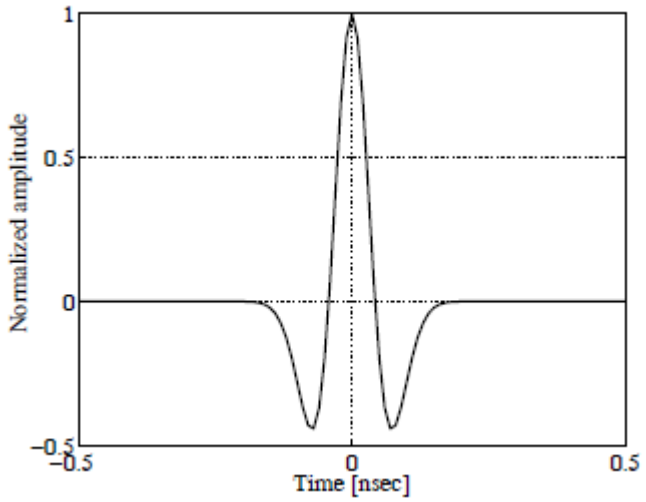

(a)

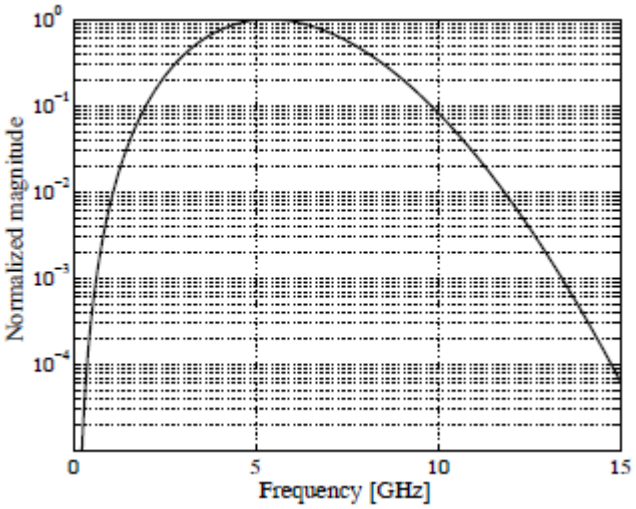

(b)

Figure 1.1: (a) idealized received UWB pulse and (b) idealized spectrum of a single received UWB pulse

2.2.3 Spectral Mask

The spectrum of a Ultra-Wideband signal is one of the important issues challenging the industry and governments for the commercial use of UWB. As UWB conspires of such a large extent of bandwidth, there are many users whose spectrum will get influenced and they need to be convinced that UWB will not result in any harmful interference to their existing

services. Hence the issue of spectrum is very important aspect of the UWB technology. Wireless communications have always been regulated to avoid interference between different users of the spectrum. Hence it is must to regulate UWB communication that there is a minimum possibility of interference with the existing licensed wireless communication system [20]. FCC regulated the unlicensed use of UWB devices with certain restrictions imposed so that no harmful interference takes place. There are many systems, whether licensed or not, are present in UHF and SHF bands. Fig 1.3 shows that several radio system existing in UHF and SHF bands.

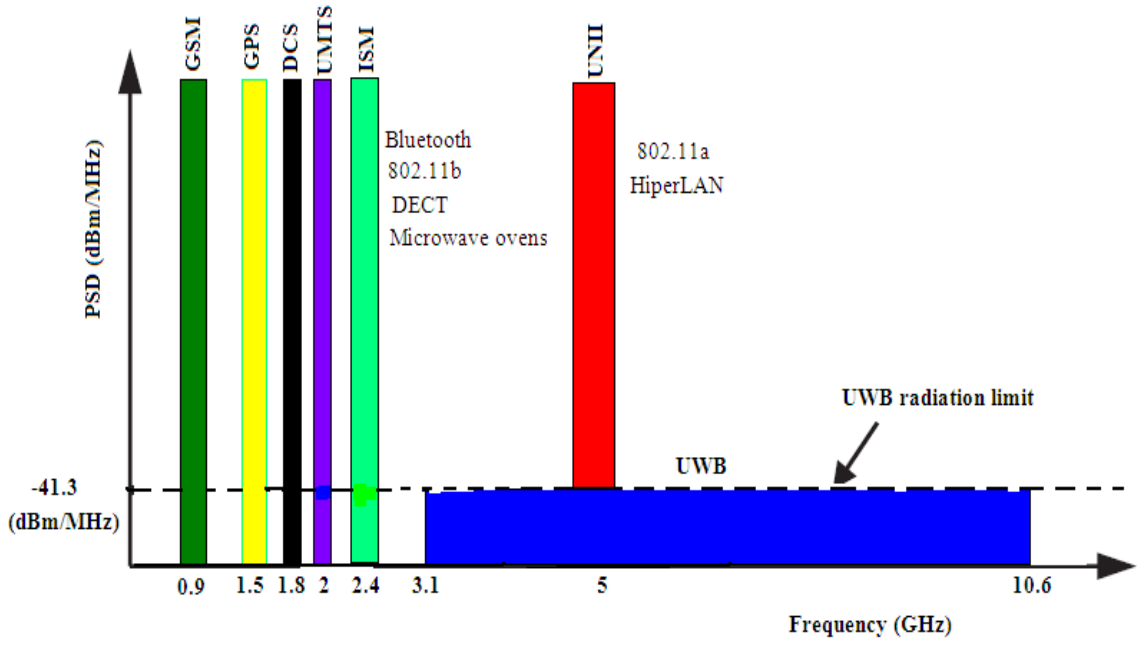

Figure 1.2: The spectrum of the UWB signals versus conventional signals

The frequency masks depend on the application and environment in which the devices are operated. Figure 3 shows the UWB spectral mask defined by FCC, for indoor UWB systems. A large continuous bandwidth of 7.5 GHz is available between 3.1 GHz and 10.6 GHz having a maximum power output of -41.3 dBm/MHz which is very less as compared to other narrow band wireless communication systems. Outside of this huge band, no intentional emissions are allowed.

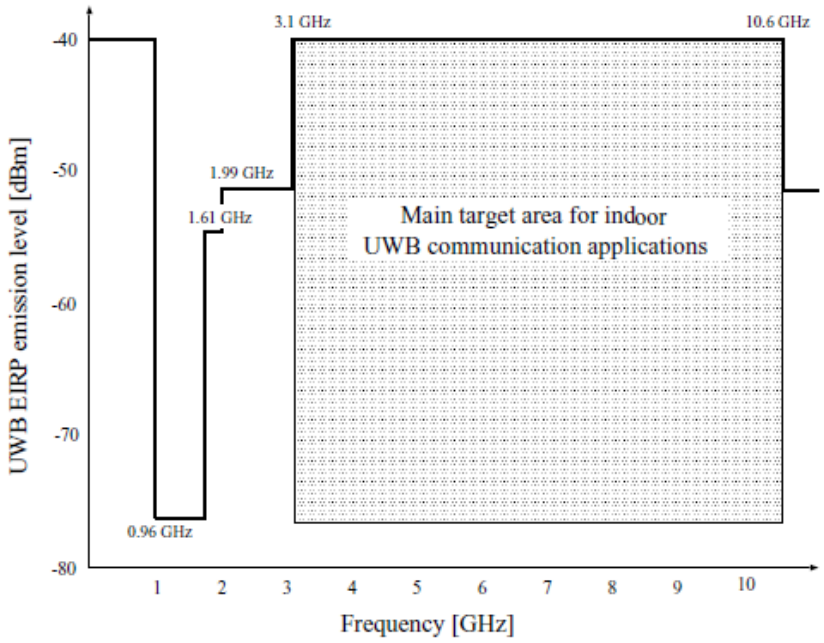

Figure 1.3: UWB spectral mask defined by FCC

2.2.4 Penetration Characteristics

One of the most key feature of the UWB communication system is the ability of these narrow pulses to easily penetrate through walls, doors, and other objects in the home and office environment. As penetration increases with increase in wavelength and UWB pulses comprises of a large range of frequencies and wavelength decreases with increase in frequency, thus the penetration capabilities of UWB come only from the lower frequency components.

2.2.5 Speed of data transmission

High data rate is one of the advantages that make it very popular for UWB communication. With this high data rate application like personal area network (PAN) where data are transmitted over short distances of 10 m or less are quite easily possible. Higher data rate (100 Mbps and up) proves useful in consumer applications like digital TV and computer

networks (wireless USB) while relatively lower data rate is useful in applications like audio streaming and other tasks that were traditionally treated by Bluetooth and infrared devices.

2.2.6 Size

The smaller size of UWB transmitter is a requirement for inclusion in today's consumer electronics. The simplest UWB transmitter could be assumed to be a pulse generator, a timing circuit and antenna. The reduced size and simple shape of UWB transmitter reduces the cost of UWB system.

2.3 Major applications of UWB Communication

2.3.1 Consumer electronics and Personal computers (PCs)

The exceptionally large available bandwidth in UWB signal forms the basis for a short-range wireless local area network with data rates approaching gigabits per second. The UWB signal also contains relatively low frequencies, thus the attenuation due to building materials is significantly lower for UWB transmissions than for millimeter wave high bandwidth solutions. Computer peripherals make use of UWB, especially when mobility is important and multiple wireless devices are utilized in a shared space. A keyboard, monitor, printer, audio speakers, mouse, microphone, and joystick are in wireless, all sending messages to the same computer from anywhere in the given range [4]. UWB pulses are used to provide extremely high data rate performance in multi-user network applications. These short duration waveforms are relatively immune to multipath cancellation effects as observed in mobile and in-building environments.

2.3.2 Position Location and Tracking

For Global Positioning Satellite System (GPS), location and positioning require the use of time to resolve signals that allow position determination to within ten of meters. Greater

accuracy is enhanced with special techniques used. Since there is a direct relationship between bandwidth and precision, therefore increasing bandwidth will also increase positional measurement precision, with UWB techniques extremely fine positioning becomes feasible, e.g., sub – centimeter and even sub-millimeter [10]. In satellite communications where wide band feeds save space and weight by supporting many communication channels with just one antenna.

2.3.3 Radar System

For radar applications, these narrow pulses provide very fine range resolution and precision distance and positioning measurement capabilities. The very large bandwidth translates into superb radar resolution, which has the capability to differentiate even between close targets. This high resolution is obtained even through lossy media such as foliage, soil and wall and floor of the buildings. Other advantages of UWB short pulses are immunity to passive interference (rain, fog, clutter, aerosols, etc) and ability to detect very slowly moving or stationary targets [11]. UWB signals enable inexpensive high definition radar. Radar will be used in areas currently unthinkable such as; automotive sensors, smart airbags, intelligent highway initiatives, etc.

2.3.4 Medical Applications

UWB signals are not influenced by clothes or blankets, and can even penetrate human body, walls, ground, ice, mud, and many interesting potential applications for UWB in medicine can be envisioned. Hospitals, Operation theatres, Home health care, intensive care units (ICU), pediatric clinics, rescue operations (to look for heart beat under ruins, or soil, or snow) are few potential areas of application [1]. A UWB sensor network frees the patient from the tangle of wired sensors. Sensors are being used in medical situation to determine pulse rate, temperature, and other critical life signs. UWB is used to transport the sensor information without wires, but also function as a sensor of respiration, heart beat, and in some instance for medical imaging. Some of the major motivations for using UWB radar and wireless communications in the field of medicine are:

(i) Non contact based Wireless Device (ii) Remote and continuous monitoring

Chapter 3

Time-Domain Heuristic Diffraction Coefficients

In this chapter, Time-Domain heuristic diffraction coefficients for UWB communication through a wedge are presented. In radio communication, the main physical phenomena for the propagation of channel are reflection, diffraction and transmission through the channel. These are the main phenomena which cause the distortion in the UWB pulse. In radio propagation of UWB signals, the diffracted field component proves to be very significant [5]. Diffracted rays are produced by incident rays which hit edges or corners. This phenomenon plays an important role when there is no LOS path between transmitter and receiver. When UWB pulses propagate through channel (free space) distortion occurs. There are two basic approaches to analysis the distortion in UWB pulse. (i) To obtain frequency-domain (FD) solution of the propagation channel and then taking IFFT of the results (ii) Direct time-domain (TD) solution. UWB signal is having a huge bandwidth, so it is more efficient to analysis UWB propagation directly in time domain because in time-domain all the frequencies are treated simultaneously. In this chapter we analysis the diffraction of UWB signals through wedge for arbitrary position of transmitter and receiver. Considering the wedge is made of dielectric lossy material, time domain formulation for diffraction coefficients for both soft and hard polarization is presented. Time domain formulation for the propagation loss and then for diffracted field at the receiver is also presented. In chapter 5, time-domain results have been validated with the inverse fast Fourier transform (IFFT) of the corresponding exact frequency domain result [18]. These Time-domain heuristic diffraction coefficients are then compared with inverse fast Fourier transform of rigorous solution for a fixed position of transmitter and receiver.

3.1 Propagation Environment

There are three possible scenario/regions which we will consider for the diffraction of UWB signal through a wedge:

(i) Deep Shadow Region,

(ii) Illumination Region,

(iii) When transmitter and receiver are on same side of wedge

3.1.1 Deep Shadow Region i.e. ($h_r < h_w$) & transmitter and receiver on either side of the wedge:

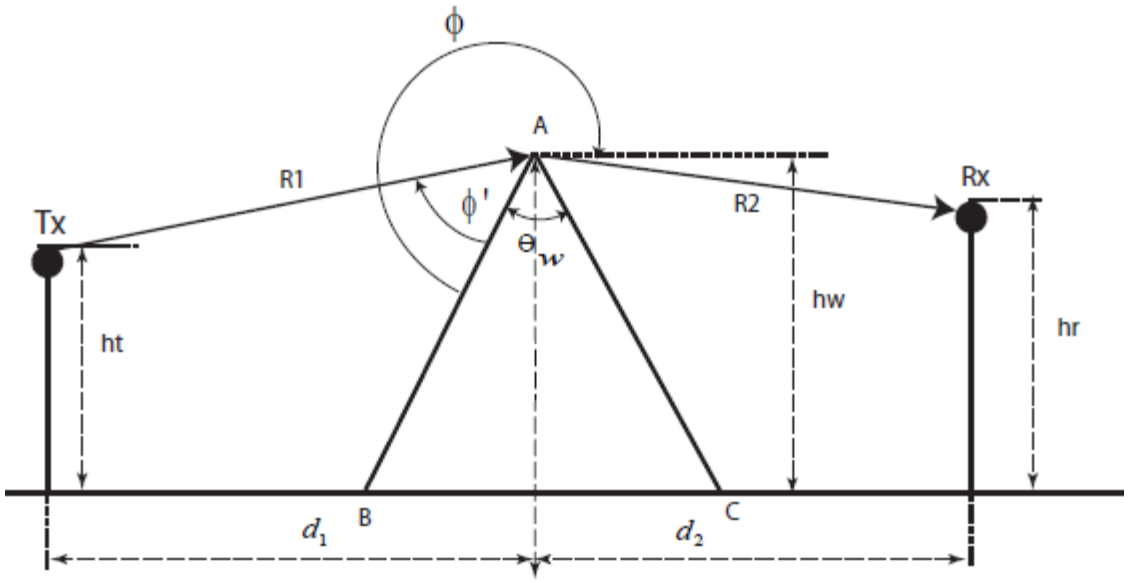

Figure 3.1: Deep Shadow Region, Non line of sight (NLOS)

Receiver (Rx) height h_r is considered lower than wedge height h_w with θ_w is considered to be wedge angle so that there is no line of sight (NLOS) communication possible between transmitter and receiver. Transmitter is positioned at distance d_1 behind the wedge distance taken from the centre of wedge and receiver (Rx) is positioned at a distance d_2 on the other side of wedge distance measure from the centre of wedge. The transmitter height h_t is considered for two cases for the shadow region i.e. (i) $h_t > h_w$ and (ii) $h_t < h_w$. As can be seen from Fig 3.1, for $h_t < h_w$, diffraction through wedge with proper ray tracing is seen.

The diffracted field depends upon the position of transmitter and receiver, with which the incidence angle and diffracted angle changes.

3.1.2 Transmitter and receiver on either side of the wedge and there is line of sight communication possible between Tx and Rx:

Receiver (Rx) height h_r is considered greater than height of the wedge h_w, such that there is a line of sight communication between transmitter and receiver, so that source(illuminates) the receiver.

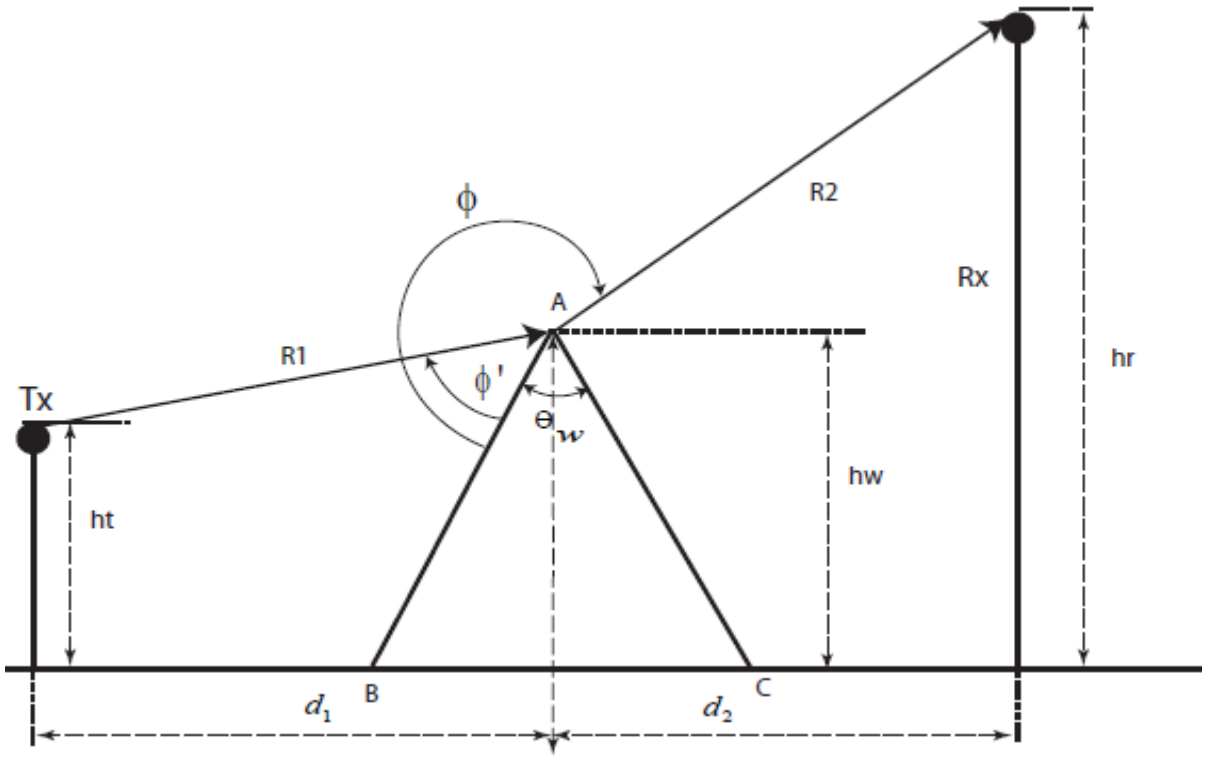

Figure 3.2: Line of Sight (LOS) Region

Transmitter is positioned at distance d_1 behind the wedge distance taken from the centre of wedge and receiver (Rx) is positioned at a distance d_2 on the other side of wedge distance measure from the centre of wedge. In this region, the diffracted field is calculated for two heights of transmitter i.e. for $(h_t > h_w)$ & $(h_t < h_w)$. The figure shows only one case i.e. when the height of transmitter is less than height of wedge.

3.1.3 When the transmitter and receiver on same side of the wedge:

The transmitter and receiver are on the same side of the wedge, in this case the diffracted field is calculated for both case with ($h_t > h_w$) & ($h_t < h_w$). The figure shows only one case i.e. when the height of transmitter is less than height of wedge.

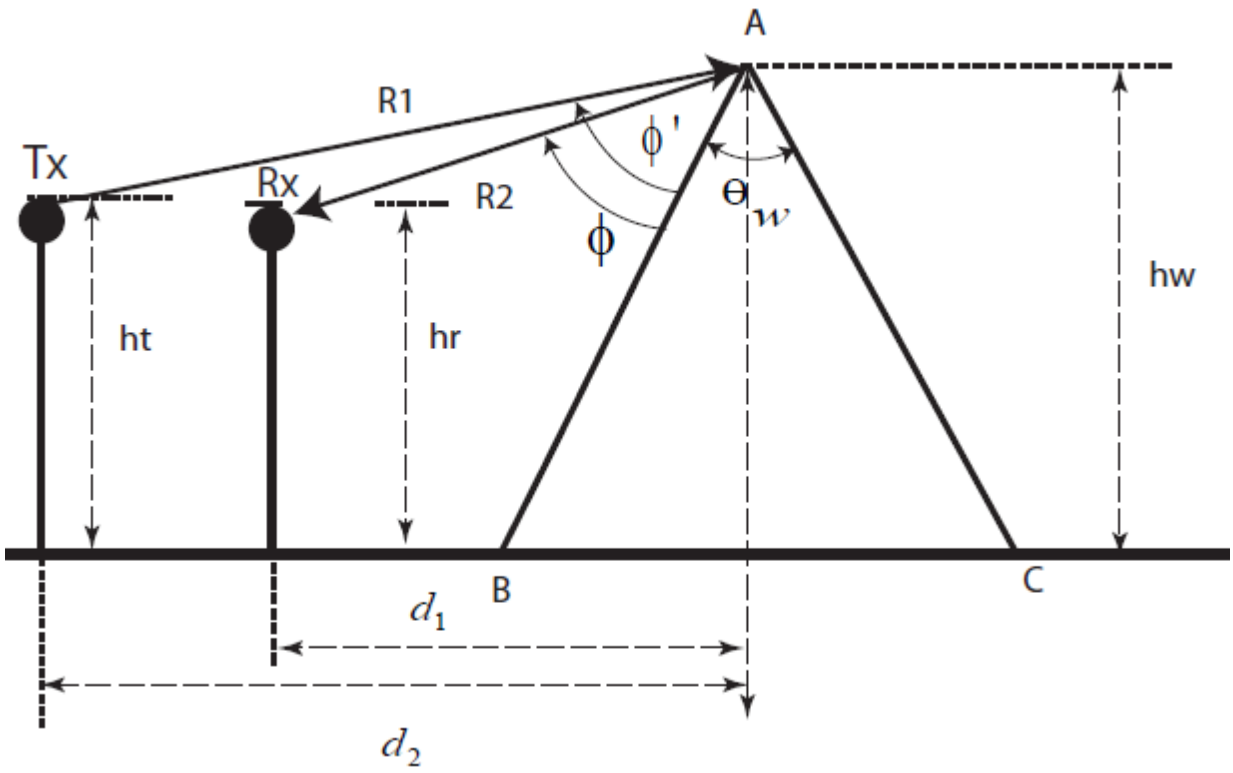

Figure 3.3: The transmitter & receiver are on the same side of the wedge.

3.2 Ray Tracing

Ray tracing algorithm is used to determine the path followed by field in wireless propagation environment. For the case of diffraction in a wedge, the transmitter is assumed to be located at a distance d_1 from the centre of the wedge and the receiver is assumed to be placed at a distance d_2 from the centre. The height of transmitter is considered to be h_t and height of receiver to be equal to h_r. The height of wedge is assumed to be equal to h_w. The wedge

angle is considered to be θ_w and exterior angle for the wedge is considered to be $n\pi$. For the calculation of diffracted field, following parameters need to be calculated which are shown in figure 3.4.

Calculation of wedge index, n:

Since the exterior angle is considered to be equal to $n\pi$ so obviously the wedge angle will be equal to $(2-n)\pi$. So the value of n entirely depends on the value of the wedge angle considered.

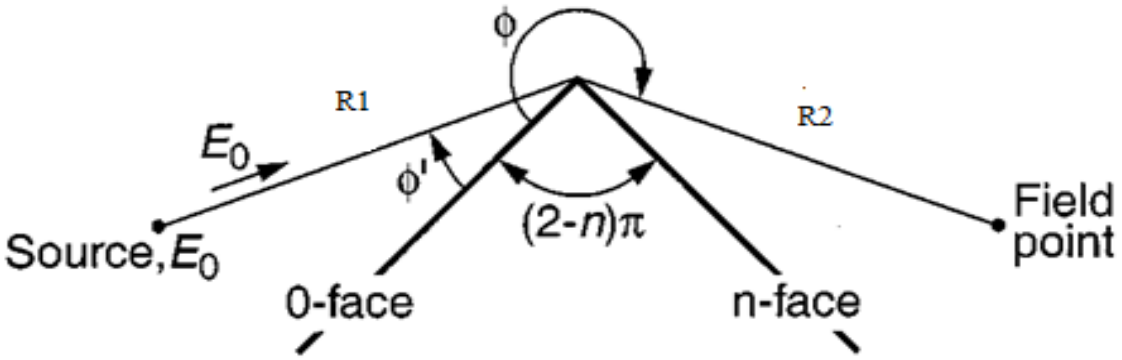

Figure 3.4: Top view of diffraction

So, $(2-n)\pi = \theta_w$

hence, $n = \frac{2\pi - \theta_w}{\pi}$.

Calculation of R_1:

R_1 is the distance between transmitter and vertex of the wedge. Calculation of R_1 depends on value of the distance of transmitter from the centre of wedge and difference in the height of transmitter and height of wedge.

i.e. $R_1 = \sqrt{(h_w - h_t)^2 + d_1^2}$

Calculation of R_2 :

R_2 is the distance between receiver and vertex of the wedge. Calculation of R_2 depends on value of the distance of receiver from the centre of wedge and difference in the height of receiver and height of wedge.

i.e. $R_2 = \sqrt{(h_w - h_r)^2 + {d_2}^2}$

Calculation of incidence angle, ϕ':

Incidence angle is defined as the angle of the ray joining the transmitter and the vertex of the wedge with respect to 0-face of the wedge. The value of incidence angle changes with the height of the transmitting antenna and whether the transmitter illuminates the 0-face or the n-face. Incidence angle also depends upon the wedge angle also. Depending upon the height and position of transmitter, there can be four cases according to which incidence angle changes.

(i) When $h_t < h_w$ and the transmitter illuminates the 0-face:

For such case, incidence angle is defined as:

Incidence angle, $\phi' = \tan^{-}(\frac{d_1}{h_w - h_t}) - \frac{\theta_w}{2}$

(ii) When $h_t > h_w$ and the transmitter illuminates the 0-face:

For such case, incidence angle is defined as:

Incidence angle, $\phi' = \pi - \tan^{-}(\frac{d_1}{h_t - h_w}) - \frac{\theta_w}{2}$

(iii) When $h_t < h_w$ and the transmitter illuminates the n-face:

For such case, incidence angle is defined as:

Incidence angle, $\phi' = 2\pi - \tan^{-}(\frac{d_1}{h_w - h_t}) - \frac{\theta_w}{2}$

(iv) When $h_t > h_w$ and the transmitter illuminates the n-face:

For such case, incidence angle is defined as:

Incidence angle, $\phi' = \frac{3\pi}{2} - \tan^{-}(\frac{h_t - h_w}{d_1}) - \frac{\theta_w}{2}$

Calculation of diffraction angle, ϕ:

Diffraction angle is defined as the angle of the ray joining the receiver and the vertex of the wedge with respect to 0-face of the wedge. The value of diffraction angle changes with the height of the receiving antenna and whether the receiver is placed on the 0-face side of the wedge or receiver is placed on the n side of the wedge. Diffraction angle also depends upon the wedge angle also. Depending upon the height and position of receiver, there can be four cases according to which diffraction angle changes.

(i) When $h_r < h_w$ and the receiver lies on the 0-face side of the wedge:

For such case, diffraction angle is defined as:

Diffraction angle, $\phi = 2\pi - \tan^{-}(\frac{d_2}{h_w - h_r}) - \frac{\theta_w}{2}$

(ii) When $h_r > h_w$ and the receiver lies on the 0-face side of the wedge:

For such case, diffraction angle is defined as:

Diffraction angle, $\phi = \frac{3\pi}{2} - \tan^{-}(\frac{d_2}{h_w - h_r}) - \frac{\theta_w}{2}$

(iii) When $h_r < h_w$ and the receiver lies on the n-face side of the wedge:

For such case, diffraction angle is defined as:

Diffraction angle, $\phi = \frac{\pi}{2} - \tan^{-}(\frac{h_w - h_r}{d_2}) - \frac{\theta_w}{2}$

(iv) When $h_r > h_w$ and the receiver lies on the n-face side of the wedge:

For such case, diffraction angle is defined as:

Diffraction angle, $\phi = \pi - \tan^{-}(\frac{d_2}{h_w - h_r}) - \frac{\theta_w}{2}$

3.3 Proposed Time-Domain Heuristic Diffraction Coefficients

The major outcome for the prediction of diffracted field came with the Pathak's Uniform geometrical theory of diffraction [6] which gave accurate result for the perfectly conducting wedges. The diffracted field for any polarization at the receiver can be calculated from the expression given below [17]:

$$E_d = \frac{E_0}{R_1} D(w)^{s,h} A(R_2) \exp(-jk(R_1 + R_2))$$

where E_d is the field at the receiver side, E_0 is the amplitude of the transmitted field, R_1 and R_2 the distance of the transmitter to the diffraction point and distance of diffraction point to the receiver respectively. K is defined as the wave number which can be defined as $\frac{w}{c}$, where c is the speed of light. $A(R_2)$ is the spreading factor and $D(w)^{s,h}$ is the diffraction coefficient where s and h denote the soft and hard polarization. $A(R_2)$ is given as:

$$A(R_2) = \sqrt{\frac{R_1}{R_2(R_1 + R_2)}}$$

A widely used diffraction coefficient D proposed by Pathak [6] is given as:

$$D_{s,h}(\phi, \phi') = \left[D1 + D2 \mp \{D3 + D4\} \right]$$

Where,

$$D_1 = \frac{-\exp[-j(\pi/4)]}{2n\sqrt{2\pi k}} \times \left[\cot\left(\frac{\pi + (\phi - \phi')}{2n} \right) F\left[kLa^{+}(\phi - \phi') \right] \right]$$

$$D_2 = \frac{-\exp\left[-j(\pi/4)\right]}{2n\sqrt{2\pi k}} \times \left[\cot\left(\frac{\pi - (\phi - \phi')}{2n} \right) F\left[kLa^{-}(\phi - \phi') \right] \right]$$

$$D_3 = \frac{-\exp\left[-j(\pi/4)\right]}{2n\sqrt{2\pi k}} \times \left[\cot\left(\frac{\pi - (\phi + \phi')}{2n} \right) F\left[kLa^{-}(\phi + \phi') \right] \right]$$

$$D_4 = \frac{-\exp\left[-j(\pi/4)\right]}{2n\sqrt{2\pi k}} \times \left[\cot\left(\frac{\pi + (\phi + \phi')}{2n} \right) F\left[kLa^{+}(\phi + \phi') \right] \right]$$

Negative sign in D is used for soft polarization while positive sign is used for hard polarization. L is the distance parameter, n is wedge index and $F(x)$ is the Fresnel transition function:

$$F(x) = 2j\sqrt{x}e^{jx} \int_{\sqrt{x}}^{\infty} e^{-j\tau^2} d\tau$$

$$L = \frac{R_1 R_2}{R_1 + R_2}$$

The $a^{\pm}$ function used in calculation of the diffraction coefficient is defined as:

$$a^{\pm}(\beta) = 2\cos^2\left[\frac{2n\pi N^{\pm} - \beta}{2} \right]$$

In which $N^{\pm}$ are the integers which most nearly satisfy the equations:

$2n\pi N^{+} - (\beta) = \pi$ and $2n\pi N^{-}(\beta) = -\pi$ with $\beta = \phi \pm \phi'$

For lossy or finitely conducting wedge, there are different heuristic diffraction coefficient proposed by Luebbers [7], Holm [8] and El-Sallabi [9]. Also it has been seen that in case of lossy wedges, in some of the regions, diffraction coefficient proposed by El-Sallabi is very accurate than given by Holm and Luebbers. Daniela [13] proposed a new diffraction coefficient by using Aidi's [14] proposed angle of incidence to provide reciprocity for arbitrary position of transmitter and receiver. But this coefficient was not reciprocal for the transmitter and receiver placed on the same side. The diffracted field in the Time-domain can be calculated from the expression given below [17]:

$$E_d = \frac{A(R_2)}{R_1} E_o * d(t)^{s,h} * \delta(t - \frac{(R_1 + R_2)}{c})$$

The term $\delta(t - \frac{(R_1 + R_2)}{c})$ does not produce any effect in the field, but it is just the time delay in the pulse. '*' denote the convolution. The time-domain formulation for the UTD diffraction coefficients in [24] and its simplified formulation is given as follows [17]:

$$d_i(t) = -\frac{Ln}{2\pi\sqrt{2c}} \frac{\sin(2a_i)}{\sqrt{t}(t + \gamma_i)}$$

With i=1,2,3,4 ; $a_i = [\pi + (\phi - \phi')] / 2n$, $a_2 = [\pi - (\phi - \phi')] / 2n$, $a_3 = [\pi - (\phi + \phi')] / 2n$,

and $a_4 = [\pi + (\phi + \phi')] / 2n$,

and $\gamma_i = \frac{2Ln^2 \sin^2(a_i)}{c}$

When $\tau \to 0$, then $\frac{1}{\sqrt{\tau}} \to \infty$, thus $d_i(t)$ approaches to infinity, there is a singularity in impulse response at $\tau = 0$. This singularity causes problems in the numerical calculation [21]. Actually, it is this singular point (at $\tau = 0$ in impulse response) that makes the main contribution to the waveform distortion. This singularity can not be directly removed by using time-window, if tried so considerable information will be lost. We then integrate the $d_i(t)$, i.e. $\int_0^t d_i(t)$. This integrity removes the singularity condition and we can convolve the signal with incident pulse. Lately, differentiation can be applied to achieve the same result.

3.3.1 Time-domain formulation for Leubbers' heuristic diffraction coefficient

Luebbers [7] modified the result by multiplying the Fresnel Reflection coefficient to the component of diffraction coefficient. With this, the coefficient became workable for the lossy dielectric wedges. The heuristic coefficient by Luebbers gives accurate result in the vicinity of the reflection boundary. Leubbers soft and hard diffraction coefficient is defined as:

$$D^{s,h} = G_0^{s,h}[D_2 + R_0^{s,h}(\alpha_0)D_3] + G_n^{s,h}[D_1 + R_n^{s,h}(\alpha_n)D_4]$$

Here, the term $G_0^{s,h}$ and $G_n^{s,h}$ are the factors used for grazing incidence which is not considered in our work, hence these factors are neglected. D_i is the UTD diffraction coefficient where i=1,2,3,4. R_0 and R_n [35,37]are the Fresnel reflection coefficient w.r.t. 0-face and n-face respectively.

Subscript s, h denote the soft and hard polarizations, for which reflection coefficient are:

$$R^s(\alpha) = \frac{\cos(\alpha) - \sqrt{\in_c - \sin^2(\alpha)}}{\cos(\alpha) + \sqrt{\in_c - \sin^2(\alpha)}}$$

And $R^h(\alpha) = \dfrac{\in_c \cos(\alpha) - \sqrt{\in_c - \sin^2(\alpha)}}{\in_c \cos(\alpha) + \sqrt{\in_c - \sin^2(\alpha)}}$

Where $\in_c = \in_r - j\dfrac{\sigma}{\omega \in_0}$ is the wedge complex relative permittivity and incidence angle α_0 and α_n are:

$\alpha_0 = \min(\phi', \phi)$, and $\alpha_n = \min(n\pi - \phi', n\pi - \phi)$

Where, $n\pi$ is the wedge exterior angle.

In the time-domain analysis, the multiplication in the formula changes to convolution all the frequency dependent term. The time-domain diffraction coefficient can be defined as:

$$d^{s,h}(t) = d_1(t) + d_2(t) + r_0^{s,h}(t) * d_3(t) + r_n^{s,h}(t) * d_4(t)$$

$d_i(t)$ is called the time-domain formulation of UTD coefficient. $r_0^{s,h}(t)$ and $r_n^{s,h}(t)$ are the time domain reflection coefficient with respect to 0-face of the wedge. Here s, h denote the soft and hard polarization, the time-domain reflection coefficient can be formulated as [37]:

$$r(t) = \mp[K\delta(t) + \frac{4k}{(1-k^2)} e^{-at}[\frac{K}{2}X + \frac{1}{2K}(1-X) - \frac{at}{4}X]]$$

where, $X = e^{-\frac{Kat}{2}}$ and $a = \frac{\tau}{2}$ where $\tau = \frac{\sigma}{\in_r}$

The leading 'minus' sign is for the hard polarization and 'plus' sign is used for the soft polarization.

For soft polarization, $k = \beta$

For hard polarization, $k = (\in_r \beta)^-$

$\beta = \frac{\sqrt{\in_r - \sin^2(\theta_i)}}{\in_r \cos(\theta_i)}$ and $K = \frac{1-k}{1+k}$

3.3.2 Time-domain formulation for Holms' heuristic diffraction coefficient

The heuristic coefficient by Luebbers gives accurate result in the vicinity of the reflection boundary but not in a deep shadow region. To improve accuracy of Luebbers heuristic coefficient, Holm further modified the original coefficient formulated by luebbers with a multiplication factors to be used in the coefficient. Holm applied the Fresnel–Kirchhoff theory to derive novel heuristic coefficients with superior performance deep in the shadow region. However this coefficient was not able to predict diffraction field accurately in the illumination region [8].

$$D^{s,h} = R_0^{s,h} R_n^{s,h} D_1 + D_2 + R_0^{s,h}(\alpha_0) D_3 + R_n^{s,h}(\alpha_n) D_4$$

All the terms were according to the Leubbers's heuristic diffraction coefficient, and the time domain diffraction coefficient formulation can be defined as:

$$d^{s,h}(t) = r_0^{s,h}(t) * r_n^{s,h}(t) * d_1(t) + d_2(t) + r_0^{s,h}(t) * d_3(t) + r_n^{s,h}(t) * d_4(t)$$

All the terms used in this heuristic coefficient have been same as of Leubber's time domain heuristic coefficient.

3.3.3 Time-domain formulation for Sallabi's heuristic diffraction coefficient:

Sallabi modified the angle definition used in the reflection coefficient and modified the Fresnel reflection coefficient too. The modified reflection coefficient was inferred from suitable formulation of the Maliuzhinets' solution [15]. In case of lossy wedges, in some of the regions, diffraction coefficient proposed by El-Sallabi is very accurate than given by Holm and Luebbers. The heuristic coefficient defined by Sallabi is given as[9]:

$$D^{s,h} = D_1 + D_2 + R^{s,h} D_3 + R^{s,h} D_4$$

where, D_i for i=1,2,3,4 are defined as per UTD coefficient and the new Reflection coefficient can be defined as [9]:

$$R^{s,h} = \frac{(1, \in_r)\tau - \sqrt{\in_r -1+\tau^2}}{(1, \in_r)\tau + \sqrt{\in_r -1+\tau^2}}$$

where, $\tau = 2\sin(\frac{\phi}{2})\sin(\frac{\phi'}{2})$

The diffraction coefficient works for both scenarios either the source faces one side or two sides of the wedge. This has influence on the definitions of ϕ and ϕ' in equation used for τ. If the source faces one side of the wedge (i.e, $\phi' < (n-1)\pi$, then the definition of the angles used are same as of incidence angle(ϕ') and diffraction angle(ϕ). If the source faces both sides of the wedge (i.e, $\phi' > (n-1)\pi$ and $\phi > (\pi - \phi')$ or, $\phi < (\pi + \phi')$ angles ϕ and ϕ' change to ($n\pi - \phi$) and ($n\pi - \phi$'), respectively, otherwise no change in the earlier definition is applied.

The time-domain heuristic coefficient can be defined as follows:
$d^{s,h}(t) = d_1(t) + d_2(t) + r^{s,h}(t) * d_3(t) + r^{s,h}(t) * d_4(t)$

$d_i(t)$ is called the time domain formulation of UTD coefficient. $r^{s,h}(t)$ is the time domain reflection coefficient with respect to 0-face of the wedge. Here s, h denote the soft and hard polarization, the time-domain reflection coefficient can be formulated as:

$$r(t) = \mp[K\delta(t) + \frac{4k}{(1-k^2)} e^{-at}[\frac{K}{2}X + \frac{1}{2K}(1-X) - \frac{at}{4}X]]$$

where, $X = e^{-\frac{Kat}{2}}$ and $a = \frac{\tau_a}{2}$ where $\tau_a = \frac{\sigma}{\in_r}$

The leading 'minus' sign is for the hard polarization and 'plus' sign is used for the soft polarization.

For soft polarization, $k = \beta$

For hard polarization, $k = (\in_r \beta)^-$

$\beta = \frac{\sqrt{\in_r -1+\tau^2}}{\in_r \tau}$ and $K = \frac{1-k}{1+k}$

3.4 Time-Domain Heuristic Diffraction Coefficients which follows Reciprocity and are symmetric

Reciprocity requires that exchanging the position of the transmitter and receiver must not change the diffraction coefficient (See Fig. 3.5) i.e. [42]

$D(\phi', \phi) = D(\phi, \phi')$

Diffraction coefficient is said to be symmetrical if the value of the diffraction coefficient remains same irrespective of the 0-face or n-face is taken as the reference face for angle measurement (see Figure 3.6) i.e. [16]

$D(\phi', \phi) = D(n\pi - \phi', n\pi - \phi)$

The Diffraction coefficients defined above were neither following reciprocity nor symmetry. So, for the consideration of arbitrarily located transmitters (sources) and receivers (observers), Aïdi and Lavergnat gave a new angular definitions [14], so that the Leubber's coefficient become reciprocal [7].

$\alpha_0 = \alpha_n = \min(\phi', \phi, n\pi - \phi', n\pi - \phi)$

With this simple modification in the definition of angles, the Leubber's diffraction coefficient was reciprocal.

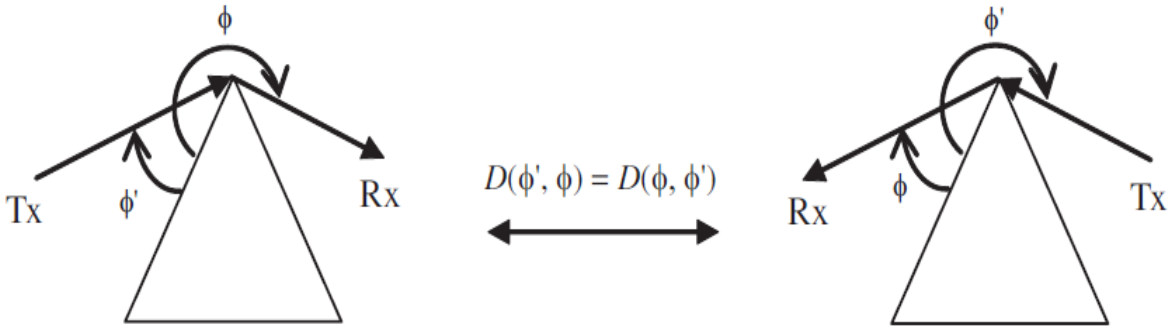

Figure 3.5: Reciprocity Condition

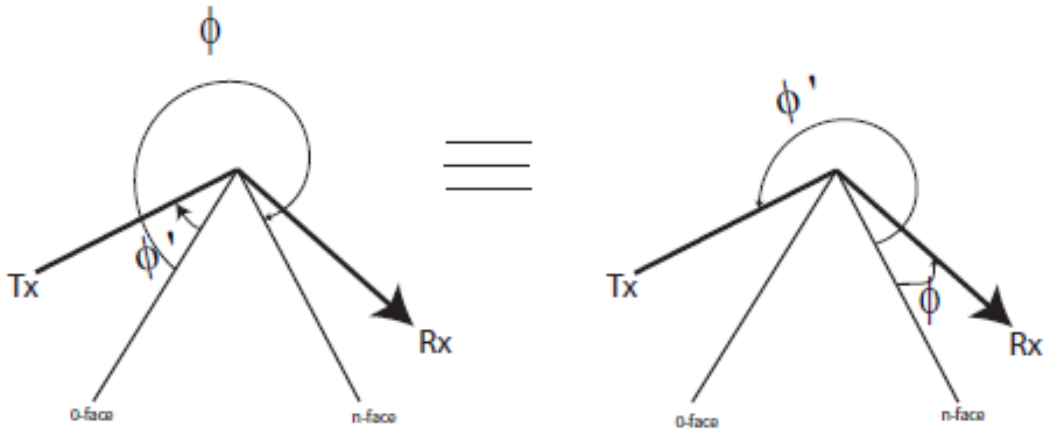

Figure 3.6: Symmetric Condition

3.4.1 Time-domain formulation for Daniela's heuristic diffraction coefficient

Daniela used the angular definition proposed by Aïdi and Lavergnat [14] to the holms' diffraction coefficient in order to make it reciprocal. For this, Daniela used the multiplying factor R_0 and R_n to D_1 when the source illuminates the 0-face of the wedge that happens for $\phi' < \frac{n\pi}{2}$. If not (i.e. $\phi' > \frac{n\pi}{2}$), multiply factor R_0 and R_n to D_2 [13]:

$$D^{s,h} = M_n^{s,h} D_1 + M_0^{s,h} D_2 + R_0^{s,h}(\alpha_0) D_3 + R_n^{s,h}(\alpha_n) D_4$$

$$M_n^{s,h} = \begin{cases} R_0^{s,h} R_n^{s,h}, \; for, \phi' < \dfrac{n\pi}{2} \\ 1, \; for,, \phi' > \dfrac{n\pi}{2} \end{cases}$$

$$M_0^{s,h} = \begin{cases} 1, \; for, \phi' < \dfrac{n\pi}{2} \\ R_0^{s,h} R_n^{s,h}, \; for,, \phi' > \dfrac{n\pi}{2} \end{cases}$$

where, the Fresnel reflection coefficient R_0 and R_n are calculated by using α_0 and α_n given by Aïdi and Lavergnat definition. The time-domain heuristic coefficient can be defined as follows:

$$d^{s,h}(t) = M_n^{s,h} * d_1(t) + M_0^{s,h} * d_2(t) + r_0^{s,h}(\alpha_0) * d_3(t) + r_n^{s,h}(\alpha_n) * d_4(t)$$

where, $M_n^{s,h} = \begin{cases} r_0^{s,h} * r_n^{s,h}, \; for, \phi' < \dfrac{n\pi}{2} \\ 1, \; for,, \phi' > \dfrac{n\pi}{2} \end{cases}$

and, $M_0^{s,h} = \begin{cases} 1, \; for, \phi' < \dfrac{n\pi}{2} \\ r_0^{s,h} * r_n^{s,h}, \; for,, \phi' > \dfrac{n\pi}{2} \end{cases}$

However, it was not reciprocal when both the Tx and Rx were on the same side of faces.

3.4.2 Symmetrical and Reciprocal Time-domain formulation heuristic diffraction coefficient:

For this, we divide the exterior angle of the wedge $n\pi$ in three regions. The regions are divided based on the reflection shadow boundary (RSB) for the 0-face and the n-face of wedge. The regions and definition of incidence angle and reflection angle is given in the table below [42].

The Time-domain formulation for the heuristic coefficient is given in the equation below:

$$d^{s,h}(t) = M_1^{s,h} * d_1(t) + M_2^{s,h} * d_2(t) + M_3^{s,h} * d_3(t) + M_4^{s,h} * d_4(t)$$

Here, $d_i(t)$ is called the time domain formulation of UTD coefficient as described earlier. The definitions of these multiplication factors are summarized in the Table 2. The definition for these reflection coefficients depends on the incidence angle used in these regions.

Region 1: $(\phi + \phi') < \pi$	$T_1 = \frac{\pi}{2} - \left\lvert \frac{\pi}{2} - \phi' \right\rvert$ $T_2 = \frac{\pi}{2} - \left\lvert \frac{\pi}{2} - \phi \right\rvert$ $\alpha_0 = \alpha_n = \min(T_1, T_2)$
Region 2: $(\phi + \phi') > \pi \cap$ $\phi \le (2n-1)\pi - \phi'$	$\alpha_0 = \min(\phi_i, \phi_d, n\pi - \phi_i, n\pi - \phi_d)$ $\alpha_n = \min(\phi_i, \phi_d, n\pi - \phi_i, n\pi - \phi_d)$
Region 3: $\phi > (2n-1)\pi - \phi'$	$T_3 = \frac{\pi}{2} - \left\lvert \frac{\pi}{2} - (n\pi - \phi') \right\rvert$ $T_4 = \frac{\pi}{2} - \left\lvert \frac{\pi}{2} - (n\pi - \phi) \right\rvert$ $\alpha_0 = \alpha_n = \min(T_3, T_4)$

Table 1: Definition of angles used for the calculation of Fresnel Reflection coefficients.

For reciprocal condition, with the above angle definition defined $M_1 \longleftrightarrow M_2$ and $M_3 = M_4$ For symmetrical property to be satisfied, we need $M_1 \longleftrightarrow M_2$ and $M_3 \longleftrightarrow M_4$. These two conditions can be satisfied simultaneously when $M_1 \longleftrightarrow M_2$ and $M_3 = M_4$. Thus, we set multiplying factors M_i , i= 1,…, 4 as described as in Table 2 [16].

Region 1,2,3	
$\phi > \phi'$	$\phi < \phi'$
$M_1 = r_0^{s,h}(\alpha_0) * r_n^{s,h}(\alpha_n)$	$M_1 = 1$
$M_2 = 1$	$M_2 = r_0^{s,h}(\alpha_0) * r_n^{s,h}(\alpha_n)$
$M_3 = r_n^{s,h}(\alpha_n)$	$M_3 = r_0^{s,h}(\alpha_0)$
$M_4 = r_0^{s,h}(\alpha_0)$	$M_4 = r_n^{s,h}(\alpha_n)$

Table 2: Multiplication factor for Time-domain coefficient

'*' denote the convolution in the table, r_0 and r_n are the Fresnel reflection coefficient in the time domain.

Chapter 4

2-D & 3-D Time-Domain Transmission Channel Modeling

In this chapter, Time-Domain modeling for transmission of UWB signals through a 2-dimensional and 3-dimensional multi-modeled obstacle is presented. In radio communication, the main physical phenomena for the propagation of channel are reflection, diffraction and transmission through the considered obstacle. These are the main phenomena which cause the distortion in the UWB pulse. In radio propagation of UWB signals, especially in non line of sight (NLOS) communication in deep shadow regions, the transmitted field component proves to be very significant[31,40]. When UWB pulses propagate through channel (free space) distortion occurs. There are two basic approaches to analysis the distortion in UWB pulse. (i) To obtain frequency-domain (FD) solution of the propagation channel and then taking IFFT of the results (ii) Direct time-domain (TD) solution. UWB signal is having a huge bandwidth, so it is more efficient to analysis UWB propagation directly in time-domain because in time domain all the frequencies are treated simultaneously [17, 21]. Considering the wedge and slab is made of low loss material, time-domain formulation for transmission coefficient for both soft and hard polarization is presented. Time-domain formulation for the propagation loss and then for transmitted field at the receiver is also presented. In chapter 5, time domain results have been validated with the inverse fast Fourier transform (IFFT) of the corresponding exact frequency domain result [32].

4.1 Propagation Environment

The propagation environment is shown in Figure 4.1 for 2-D scenario and in Figure 4.2 for 3-D scenario, in which a single dielectric wedge is followed by a dielectric slab. The parameters $r_i, i = 1,2...,5$ are the distances traversed by the transmitted field through the structure from the transmitter (Tx) up to the receiver (Rx). Angles $\theta_1, \theta_3, \theta_5, \theta_7$ are the

incidence angles with $\theta_2, \theta_4, \theta_6, \theta_8$ as the angles of refraction at points 'P', 'Q', 'R' and 'S' respectively and a_i is the internal wedge angle. The parameters h_t and h_r are the heights of

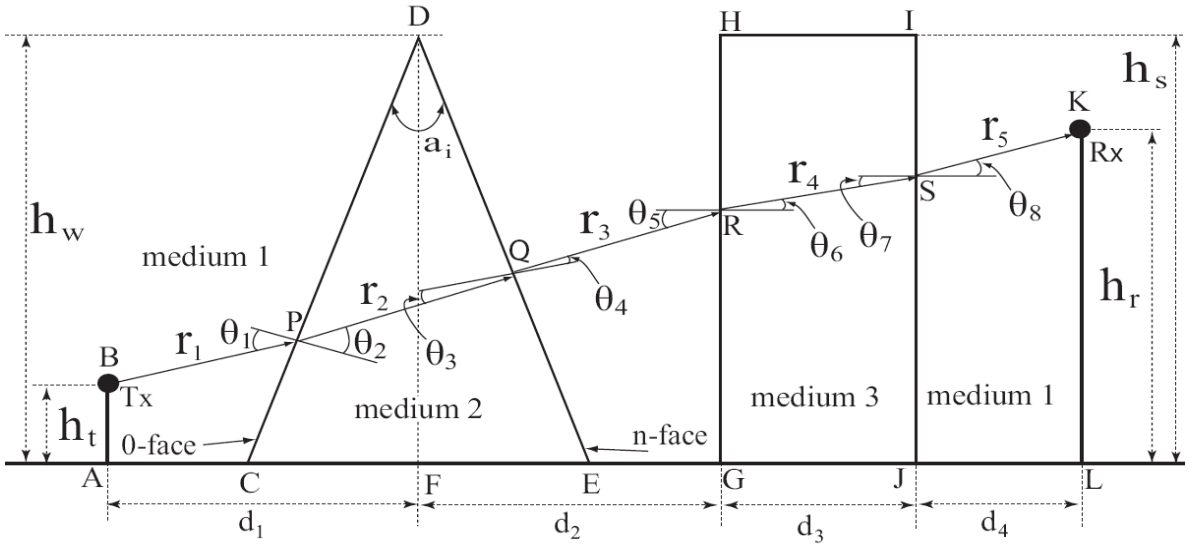

Figure 4. 1. Transmission through a 2-d scenario i.e. dielectric wedge followed by a dielectric slab

the transmitter and the receiver, h_w is the height of the wedge and h_s is the height of the slab. Tx is at a distance d_1 from the wedge, d_2 is distance between wedge and slab, d_3 is width of slab and d_4 is distance between slab and Rx and for the 3-D scenario, z_r is the receiver position w.r.t. transmitter along z-axis.

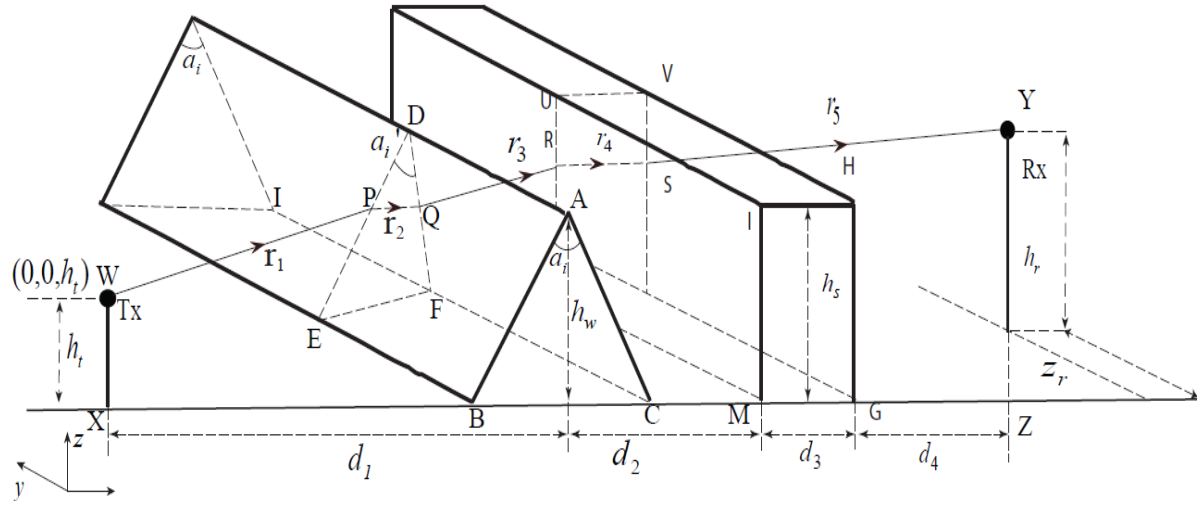

Figure 4. 2. Transmission through a 3-d scenario i.e. dielectric wedge followed by a dielectric slab

4.2 Ray Tracing

4.2.1 Algorithm to determine the transmission path through a 2-D Scenario

Considering the transmitter position as a origin, the position of receiver can be defined as (xr,0). The height of transmitter and receiver is considered to be h_t and h_r resp. The obstacle considered is a multi-modeled obstacle – dielectric wedge followed by dielectric slab:-

- Considering the left side of wedge, choose an arbitrary point with incident angle θ_1 of the incident ray from Tx, with respect to normal at 0-face of the wedge. For each of the chosen point, compute the angles θ_3 and true refracted angle θ_2, θ_4 .

- Also compute the coordinates of points P, Q, (intersection points of transmitted path along the wedge).

- Now considering the left side of slab, compute the angle θ_5 made at intersecting point R with respect to normal to the left side of slab. For this, compute the angles θ_7 and true refracted angles θ_6, θ_8.

- Also compute the coordinates of points P, Q,(intersection points of transmitted path along the slab).

- Next compute the y coordinate of the transmitted path at a receiver point. Let this value be $h_{estimate}$. The difference $\Delta h = (h_r - h_{estimate})$ is stored in a vector $\overline{error}$ (h_r is the height of receiving antenna).

- Repeat this process for each sample point of the incident angle on the left side of first layer of the wall and store the error value in vector $\overline{error}$.

- Find the minimum error from the vector $\overline{error}$. If this minimum error is less than the desired threshold, then the transmission path corresponding to that error's value is the desired path otherwise the step size $\Delta\theta_i$ is reduced till the minimum error is less than the set threshold error and this way best approximate path is obtained.

4.2.2 Proposed algorithm to determine the transmission path through a 3-D Scenario

Considering the transmitter position as a origin, the position of receiver can be defined as (x_r ,0, z_r). The height of transmitter and receiver is considered to be h_t and h_r resp. The obstacle considered is a 3-dimensional multi-modeled obstacle – 3-d dielectric wedge followed by 3-d dielectric slab:-

- 3-Dimensional problem is converted into 2- Dimensional problem by considering the 3-D scenario as a collection of various 2-Dimensional planes, connecting transmitter to receiver.
- The new wedge angle $a_i^{'}$, the new distances z_1, z_2, z_3 and z_4 are calculated with respect to the location of the receiver along the z-direction.
- z_1 is the distance from the centre of wedge to the transmitter, z_2 is distance between wedge and slab, z_3 is width of slab and z_4 is distance between slab and Rx.
- Now, with this new wedge angle and new distances, the same procedure as explained above for the above 2-D problem is used for ray tracing.

4.3 Proposed Transmission Model

4.3.1 TD transmission coefficient

The actual refracted angle across conductor-dielectric interface is given by [3]

$$\psi_t(\omega) = \tan^{-1}\{t(\omega)/q(\omega)\} \quad (1)$$

with $t(\omega) = \beta_1(\omega)\sin\theta_1$ and $q(\omega) = s(\omega)\{\alpha_2(\omega)\sin\zeta(\omega) + \beta_2(\omega)\cos\zeta(\omega)\}$.

where α_i and β_i are the attenuation constant and phase shift constant of i^{th} medium. θ_1 is the incident angle and $\cos\{\theta_2(\omega)\} = s(\omega)\exp[j\zeta(\omega)]$ with $\theta_2(\omega)$ as the complex refracted angle.

From (1) it is clear that the true refraction angle is also frequency dependent in nature, which means that for different frequency components of the UWB signal, the true real angles of refraction are different. However for low-loss dielectric obstacles (i.e. $\sigma/\omega\varepsilon << 1$), the different true refracted angles reduce to an effective, constant real angle [12]. Thus the real

refracted angle ψ_t can be treated as constant and frequency independent, to obtain the approximate analytical TD transmission coefficients. Now for hard polarization case, transmission coefficient while propagating from conductor to dielectric medium, is given by [35, 37, 38]

$$\gamma_h(t) \approx \delta(t) - r_h(t) \tag{1}$$

$$r_h(t) = \left[K_h \delta(t)\right] + \frac{4k_h}{\left(1-k_h^{\,2}\right)} e^{-pt}\left[\frac{K_h}{2} X_h + \frac{(1-X_h)}{2K_h} - \frac{(pt)X_h}{4}\right] \tag{2}$$

with $X_h = e^{-\left(\frac{K_h pt}{2}\right)}, K_h = \left(\frac{1-k_h}{1+k_h}\right), k_h = (\cos\theta_i / \cos\psi_t)(1/\sqrt{\varepsilon_{r2}})$, and $p = \tau/2$ with $\tau = \sigma/\varepsilon_2$.

where, ε_2 and εr_2 are dielectric permittivity and relative dielectric permittivity of the dielectric medium respectively. The TD transmission coefficient for a soft polarized wave propagating from conductor to dielectric medium is given as

$$\gamma_s(t) \approx \left[\delta(t) - r_s(t)\right]\left(\frac{\cos\theta_i}{\cos\psi_t}\right) \tag{3}$$

where, $r_s(t) = K_s\delta(t) + \frac{4k_s}{\left(1-k_s^{\,2}\right)} e^{-pt}\left[\frac{K_s}{2} X_s + \frac{(1-X_s)}{2K_s} - \frac{(pt)X_s}{4}\right]$ with $X_s = e^{-\left(\frac{K_s pt}{2}\right)}$,

$K_s = \left(\frac{1-k_s}{1+k_s}\right)$, $k_s = \left(\cos\psi_t / \cos\theta_i\right)\left(1/\sqrt{\varepsilon_{r2}}\right)$.

4.3.2 Transmitted field through the propagation environment

The FD expression for the transmitted field at Rx through the structure shown in Fig. 1 is given by [12,40]

$$E_{RX}(\omega) = \left(E_i(\omega)/r_{total}(\omega)\right)\left(\prod_{i=1}^{4} T_{i,s,h}(\omega)\right)\left(\exp\left(-jk_0 r_1\right)\prod_{j=2}^{5}\exp\left\{-\left(\alpha_{ej}(\omega) + j\beta_{ej}(\omega)\right)\right\}\right) \tag{4}$$

with,

$$r_{total}(\omega) = \sum_{i=1}^{5} r_i \text{ and } T_{total,s,h}(\omega) = \prod_{i=1}^{4} T_{i,s,h}(\omega)$$

where $T_{i,s,h}(\omega), i = 1,2...,4$ are the FD transmission coefficients with respect to points 'P', 'Q', 'R' and 'S' (See Figure 4.1 and 4.2). $\alpha_{ej}(\omega), \beta_{ej}(\omega)$ are total effective attenuation constants and phase shift constants for different j^{th} regions [12]. Actual FD path-loss expression from (5) is given by

$$L_{total,s,h}(\omega) = \left(\exp(-jk_0 r_1) \prod_{j=2}^{5} \exp\left\{ -\left(\alpha_{ej}(\omega) + j\beta_{ej}(\omega) \right) \right\} \right) \tag{5}$$

Now the corresponding TD expression for the received field at Rx based on the FD transmission model of [42] is as follows

$$e_{RX}(t) \approx \left(\frac{e_i(t)}{r_{total}} \right) * \Gamma_{1,s,h}(t) * \Gamma_{2,s,h}(t) * \Gamma_{3,s,h}(t) * \Gamma_{4,s,h}(t) * l_{total,s,h}(t) \tag{6}$$

with '$*$' representing the convolution operator, $\Gamma_{1,s,h}(t) * \Gamma_{2,s,h}(t) * \Gamma_{3,s,h}(t) * \Gamma_{4,s,h}(t) = \Gamma_{total,s,h}(t)$ is the TD counterpart of $T_{total,s,h}(\omega)$, $l_{total,s,h}(t)$ [37,39] is the TD counterpart of $L_{total,s,h}(\omega)$. The TD expressions for $\Gamma_{i,s,h}, i = 1,2...,4$ can be obtained using (2) and (4) for different polarizations.

For loss tangent much less than unity $(\sigma / \omega\varepsilon << 1)$, the FD path-loss expression (6) reduces to the following approximate form with constant values of angles of refraction and along a single effective path for transmission:

$$L_{total,s,h}(\omega) \approx \exp\left(-jk_0(r_1 + r_3 + r_5)\right) \exp\left[-j\omega\sqrt{\mu\varepsilon} \left(1 + \frac{\sigma}{2j\omega\varepsilon} \right) \left\{ r_2 + \left(d3 \sqrt{\frac{\varepsilon_r}{\varepsilon_r - \sin^2\theta_5}} \right) \right\} \right] \tag{7}$$

Here $r_1 + r_3 + r_5$ is the total distance travelled by the field in free space. ε and σ are the parameters of the dielectric mediums in Fig. 1 (assuming same for wedge and slab). The term $l_{total,s,h}(t)$ in (7) is then given by

$$l_{total,s,h}(t) \approx \exp\left[-\sqrt{\mu/\varepsilon}\left(\sigma/2\right)\left\{r_2+\left(d3\sqrt{\frac{\varepsilon_r}{\varepsilon_r-\sin^2\theta_5}}\right)\right\}\right]$$
$$\delta\left[t-\sqrt{\mu\varepsilon}\left\{r_2+\left(d3\sqrt{\frac{\varepsilon_r}{\varepsilon_r-\sin^2\theta_5}}\right)\right\}\right]*\delta\left(t-\frac{r_1+r_3+r_5}{c}\right) \quad (8)$$

This approximated TD path-loss expression will be used in (7) to compute the TD transmitted field and the accuracy will be proved by the comparison of TD transmitted field with the IFFT of the exact FD results, as shown in next chapter.

Chapter 5

SIMULATIONS & RESULTS

In this section, numerical simulation results of diffracted and transmitted field for different propagation environments are presented. In all results the Gaussian doublet pulse is used as the excitation UWB signal. The expression of UWB signals in time domain can be given as

$$s(t) = \left(\frac{1}{\tau}\right)\left(\sqrt{\frac{\tau}{3\sqrt{\pi/2}}}\right)\left(1-\frac{2t^2}{\tau^2}\right)\exp\left(-\frac{t^2}{\tau^2}\right)$$

Where τ is the full width half maximum pulse duration with a value of 0.1 ns. The Fourier transform of $s(t)$ is given as

$$S(f) = 2\times\sqrt{\pi}\times\sqrt{\frac{\tau}{3\sqrt{\pi/2}}}\times\left(\pi^2\tau^2 f^2\right)\times e^{-\pi^2\tau^2 f^2}$$

5.1 Comparative Analysis of Different Heuristic Diffraction Coefficients

Through all the propagation media considered for the diffraction case, a dielectric wedge of dielectric relative permittivity $\in_r = 5$ and conductivity $\sigma = 0.016$ S/m is considered. The wedge angle=10^o and height of the transmitter is considered to be equal to 1m. The height of wedge is considered equal to 2m. In this work, all the comparative analysis is done for the three different propagation media explained in chapter 3.1. All the different heuristic coefficients are compared with the inverse fast Fourier transform of the Rigorous solution.

For Deep Shadow Region:

For this propagation scenario, the height of receiver is taken to be equal to 1m, and the distance of transmitter and receiver from centre of the wedge is equal to 2m. In case of hard polarization, the heuristic time-domain coefficient for deniela and sallabi is giving result very close to that of Rigorous Solution (as can be seen in Fig 5.1).

But for the Soft polarization, time-domain coefficient for S.k.S. heuristic coefficient is giving solution very close to the Rigorous Solution (as can be seen from fig. 5.2).

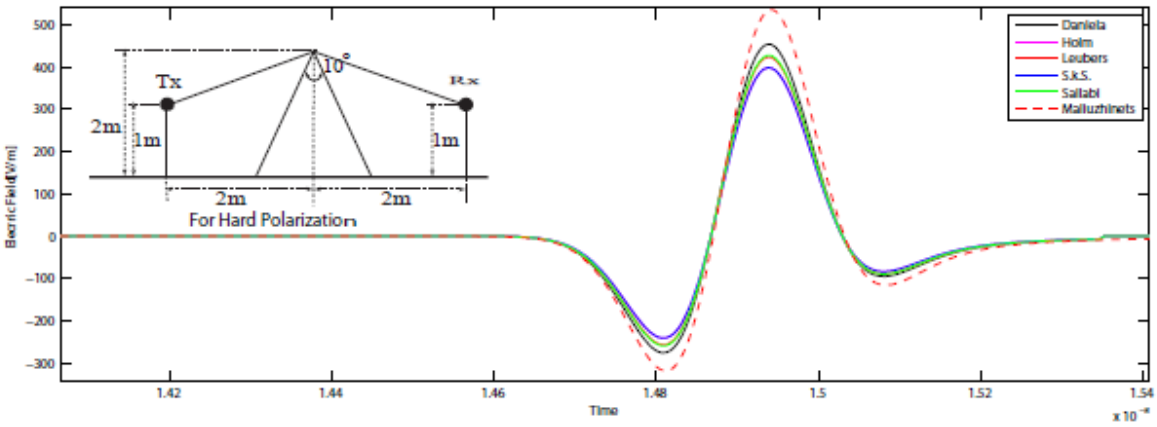

Figure 5.1: Comparison of different Time-domain diffraction coefficients for Deep shadow region for Hard polarization.

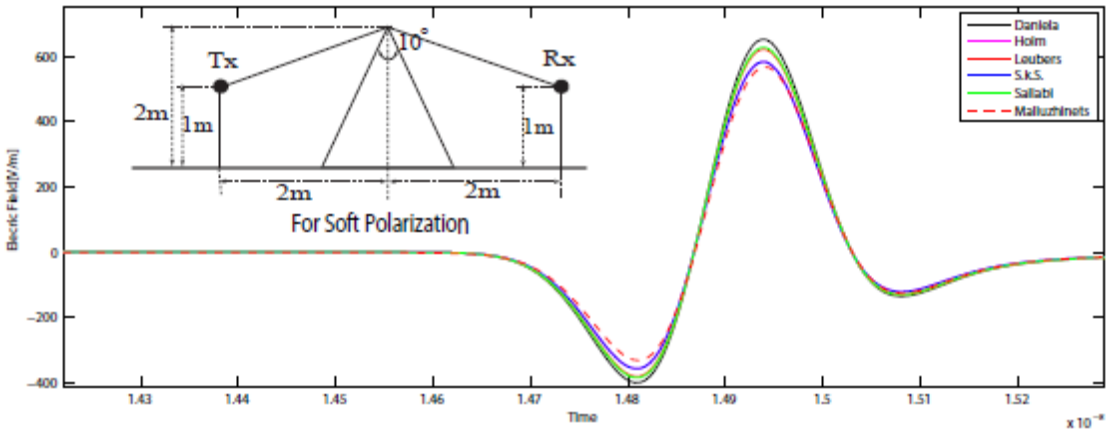

Figure 5.2: Comparison of different Time-domain diffraction coefficients for Deep shadow region for Soft polarization.

For LOS Region:

For this propagation scenario, the height of receiver is taken to be equal to 4m, and the distance of transmitter is equal to 2m and receiver is equal to 1m both considered from centre of the wedge. In case of hard polarization, the heuristic time-domain coefficients for sallabi and deniela is giving result very close to that of Rigorous Solution (as can be seen from fig. 5.3).

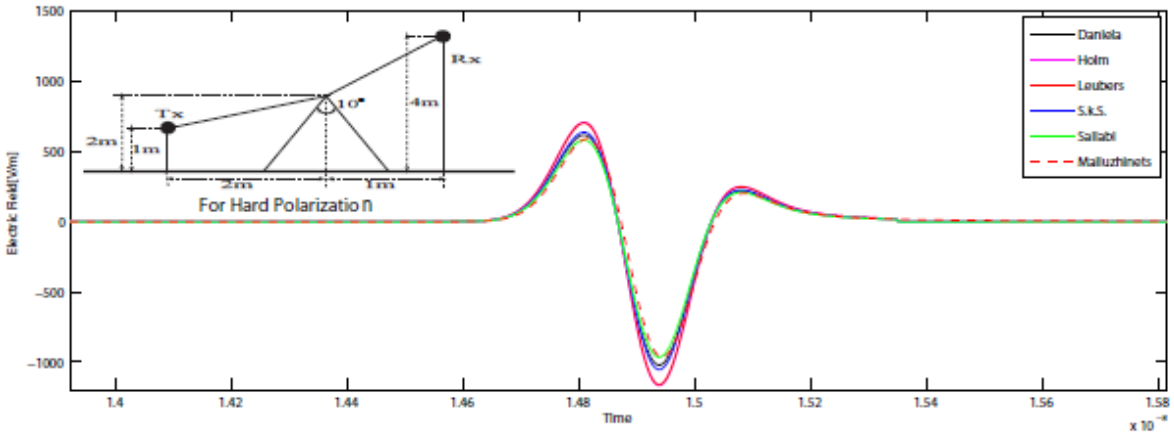

Figure 5.3: Comparison of different Time-domain diffraction coefficients for LOS region for Hard polarization.

But for the Soft polarization, time-domain coefficient for S.k.S. and Daneila's heuristic coefficient is giving solution very close to the Rigorous Solution as can be seen from fig. 5.4.

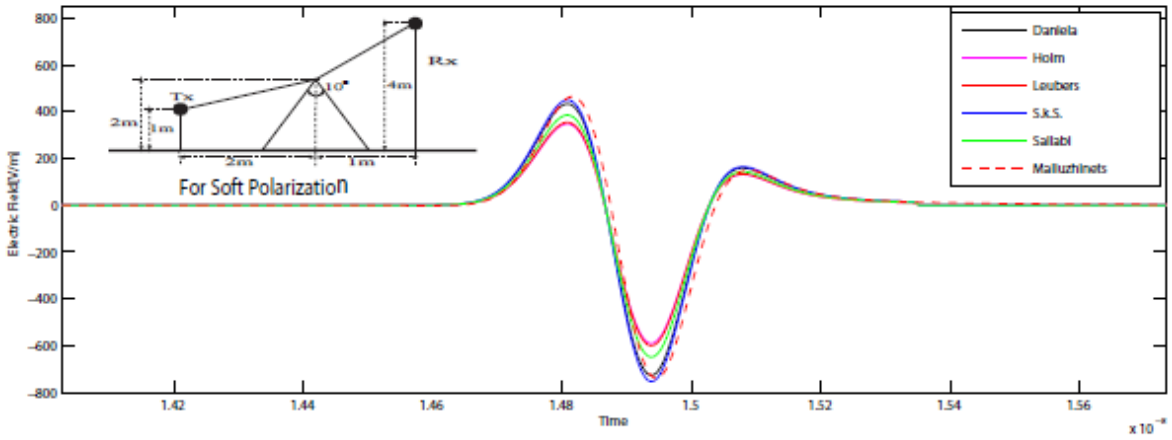

Figure 5.4: Comparison of different Time-domain diffraction coefficients for LOS region for Soft polarization.

When the Tx and Rx are on same side of wedge:

For this propagation scenario, the height of receiver is taken to be equal to 1m, and the distance of transmitter is equal to 2m and receiver is equal to 1m both considered from centre of the wedge. For the case of Hard polarization, the field predicted by Leubber and Sallabi is very much incorrect in accordance to the result of Rigorous Solution. The field predicted by

the time-domain solution of S.K.S is very much approximate to the result obtained from Rigorous solution.

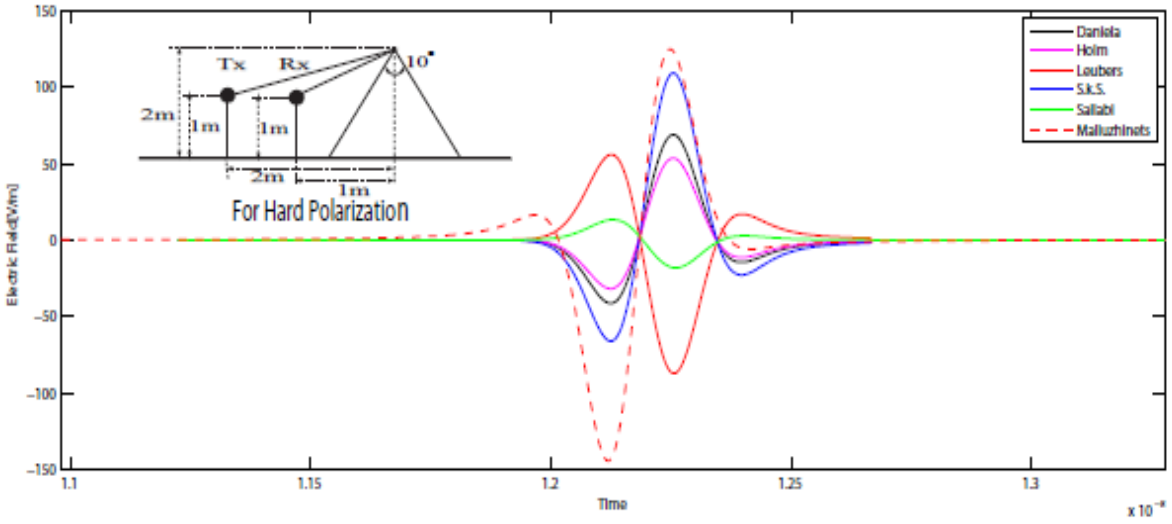

Figure 5.5: Comparison of different Time-domain diffraction coefficients for when Tx & Rx are on same side for Hard polarization.

For the Soft polarization, the field predicted by Leubber and Sallabi is very high compared to Rigorous Solution. The field predicted by time-domain diffraction coefficient of S.K.S is in accordance to the Rigorous Solution.

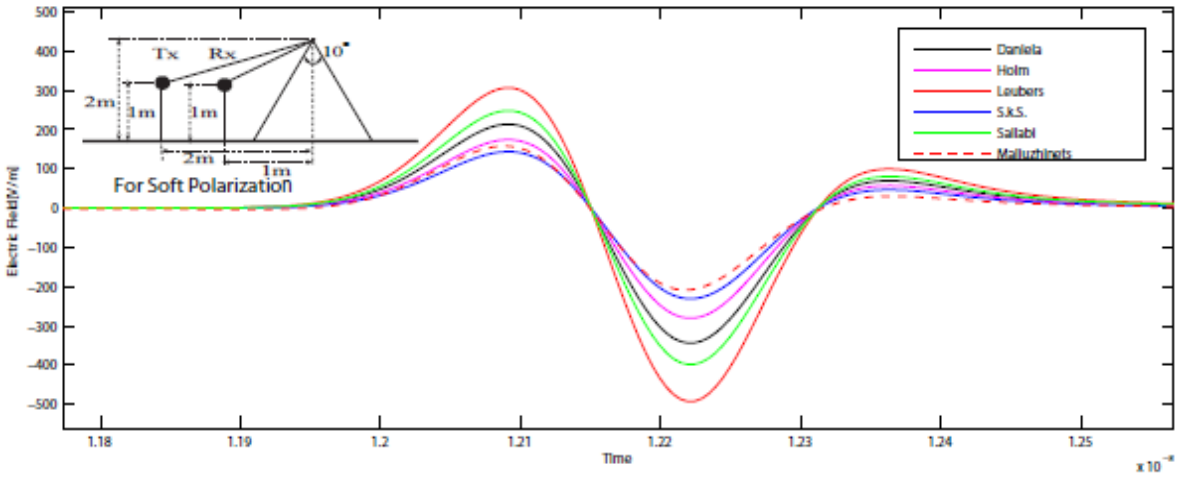

Figure 5.6: Comparison of different Time-domain diffraction coefficients for when Tx & Rx are on same side for Soft polarization.

5.2 Symmetric & Reciprocal Time-Domain Diffraction Coefficient

Symmetric

The Deep shadow region is considered to validate the symmetric property of the heuristic coefficient. In the first case, the angle measurement is done with respect to 0-face and in the second case; it is measured with respect to the n-face. The result is shown in Fig. 5.7. Both the hard and soft polarization is considered. The Electric Field obtained through these two angle measurements is exactly overlapping.

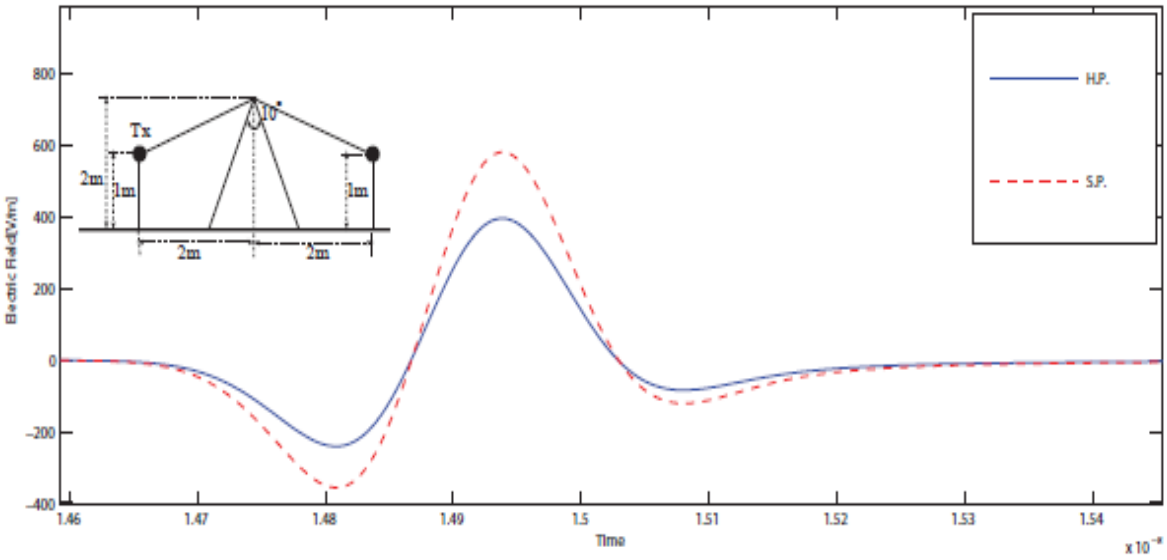

Figure 5.7: Comparison of Diffracted Field obtained from the angle measurement from 0-face and n-face for both polarizations.

Reciprocal

The Deep shadow region is considered to validate the reciprocity property of the heuristic coefficient. The transmitter and receiver positions are interchanged with respect to each other. The result is shown in Fig. 5.8. Both the hard and soft polarization is considered. The electric field obtained is exactly overlapping for both the polarizations when the transmitter and receiver positions are interchanged.

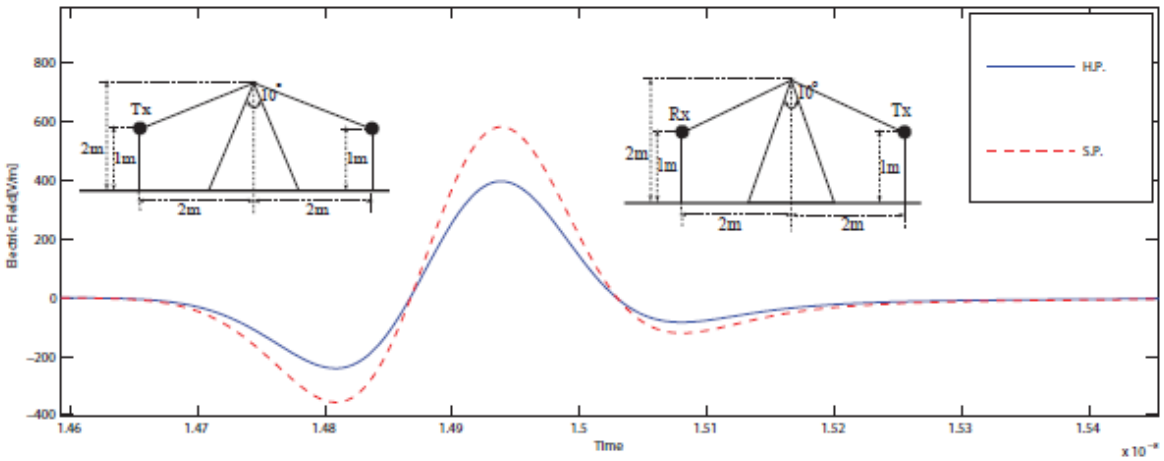

Figure 5.8: Comparison of diffraction field obtained from interchanging the position of Tx & Rx for both polarizations.

5.3 Time-Domain Approximation of Transmitted Field through Multi-modeled Obstacle

We have considered the obstacle made up of low loss dielectric materials with relative magnetic permeability as unity and relative dielectric permittivity and conductivity are chosen such that the resulting loss tangent values are in accordance with that of dry-wall, Wood and Glass (see Table 3). Table 3 shows the electromagnetic properties of the considered materials.

Table 3: Electromagnetic properties of different dielectric materials

Material	Relative Permittivity	Conductivity (S/ m)
Wood	2	0.01
Drywall	2.4	0.004
Glass	6.7	0.001

In case of FD analysis of transmission of UWB signal through the considered obstacle, first the frequency components contributing to total transmitted field at receiver are distinguished. As we have discussed earlier (chapter 4) that different frequency components of the transmitted signal follow different paths after refraction up to Rx. So frequency components reaching within an error of 10^{-5} m with respect to receiver are considered as reaching exactly

at receiver. Considering only these frequency components the transmitted field at receiver is calculated. To obtain the reference transmitted field, the IFFT of this result is also computed. In TD analysis, by using a ray tracing algorithm (see section 4.2 of chapter 4) based on low loss approximation, a single effective path of the transmitted field through building is traced. The transmitted field along that effective path is calculated in TD. For validation of the proposed solution, The TD transmitted filed results are compared with reference IFFT-FD results.

In this section, our goal is to compare the proposed TD solution with conventional IFFT-FD method. Fig. 5.9 shows the transmitted field through the propagation environment discussed in chapter 4, for both hard and soft polarizations. The transmitted field at Rx suffers no distortion in shape in comparison to the shape of the excited UWB pulse. This is because of small magnitude of the loss tangent with respect to unity. However, the amplitude of the transmitted field is attenuated because of the transmission loss through the dielectric mediums.

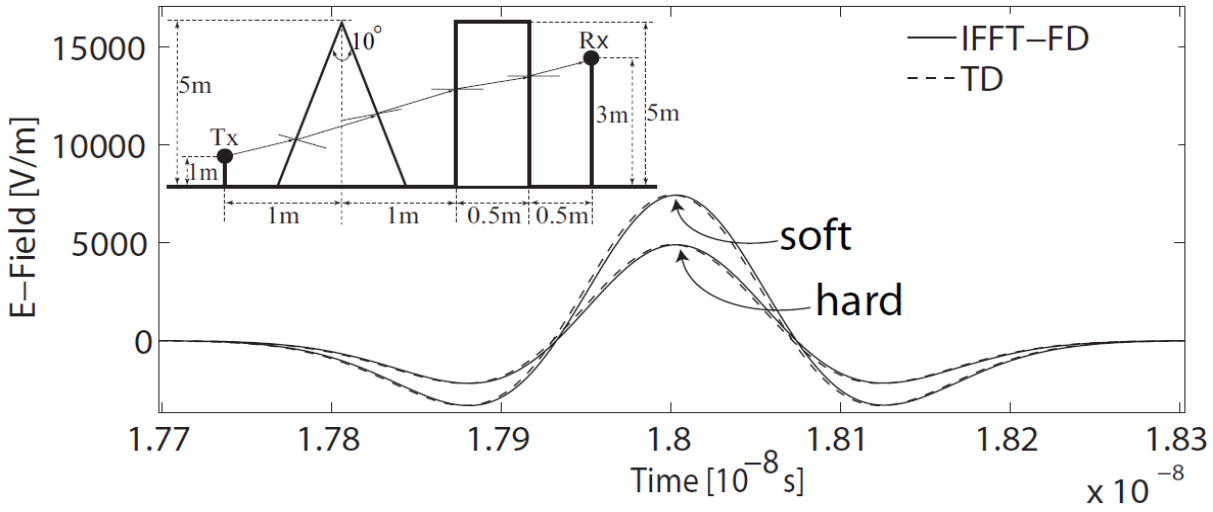

Figure 5.9**:** Transmitted field through 2-D ‘dielectric wedge followed by a dielectric slab’, with glass.

The TD results for the transmitted field for both the polarizations are in excellent agreement with corresponding IFFT of exact FD results, thus providing validation to the proposed TD solution. In MATLAB simulation, it is observed that some offset value in time-axis still remains between TD and IFFT-FD results and that was noted due to MATLAB limitations. In all the following results, this offset has been compensated. Fig.5.10 shows the effect of

varying Rx position (changing distance d_4 in Fig. 4.1) on transmitted field at the receiver. Transmitted field gets more attenuated as Rx moves away from the obstacles. The results for soft and hard polarized fields come closer to each other as the distance d_4 increases. Also the TD results match closely with the IFFT-FD results.

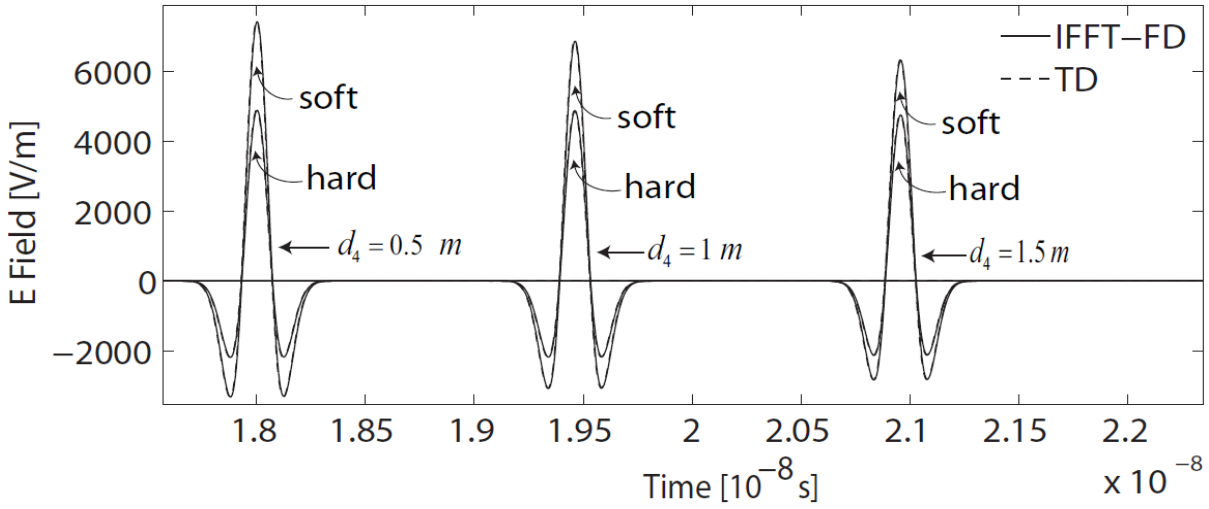

Figure 5.10: Transmitted field through 2-D 'dielectric wedge followed by a dielectric slab' for different receiver positions, with glass.

Fig. 5.11 shows transmitted field at the receiver for different dielectric materials. The TD results are in good agreement with the IFFT-FD results. It can be seen that as the value of loss tangent decreases, a better agreement is achieved between the TD and IFFT-FD results.

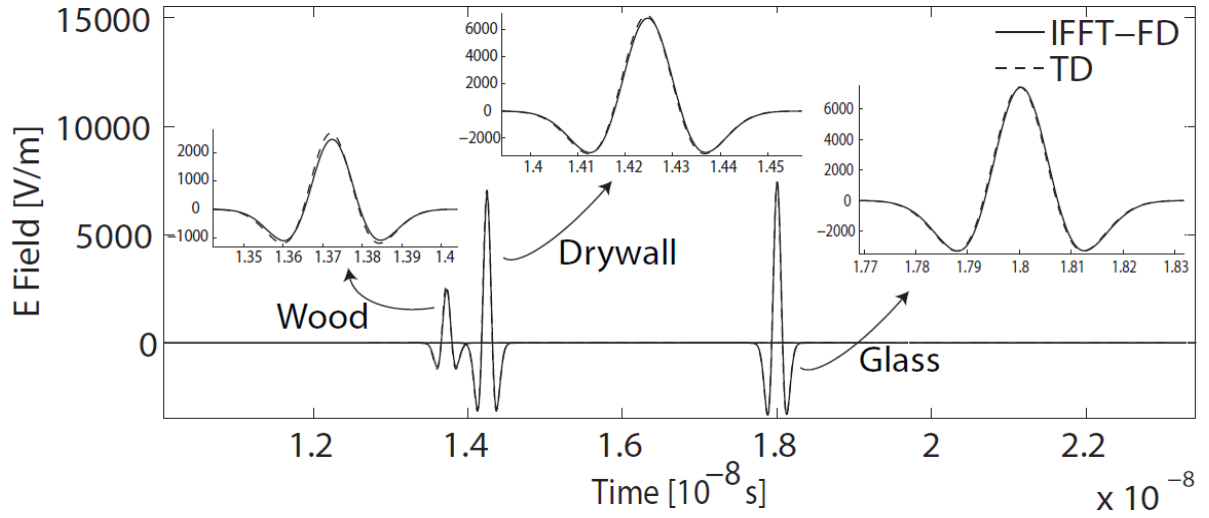

Figure 5.11**:** Transmitted field through 2-D 'dielectric wedge followed by a dielectric slab' for different dielectric materials, with wood, drywall and glass.

Fig. 5.12 shows the transmitted field through the 3-D propagation environment discussed in chapter 4, for both hard and soft polarizations. In this the position for receiver with respect to transmitter along the z-axis is taken to be 2m.

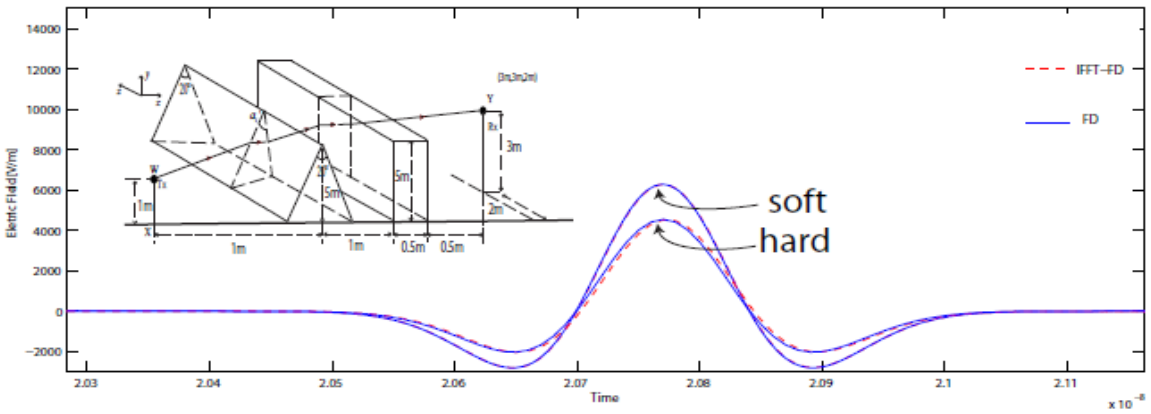

Figure 5.12**:** Transmitted field through 3-D 'dielectric wedge followed by a dielectric slab', with glass with z_r =2m.

Fig. 5.13 shows the effect of varying Rx position (changing distance z_r in Fig. 4.2) on transmitted field at the receiver. Transmitted field gets more attenuated as Rx moves along the z-axis same as for 2-D case as the distance of receiver increases in both cases. The results for soft and hard polarized fields come closer to each other as the distance z_r increases. Also the TD results match closely with the IFFT-FD results.

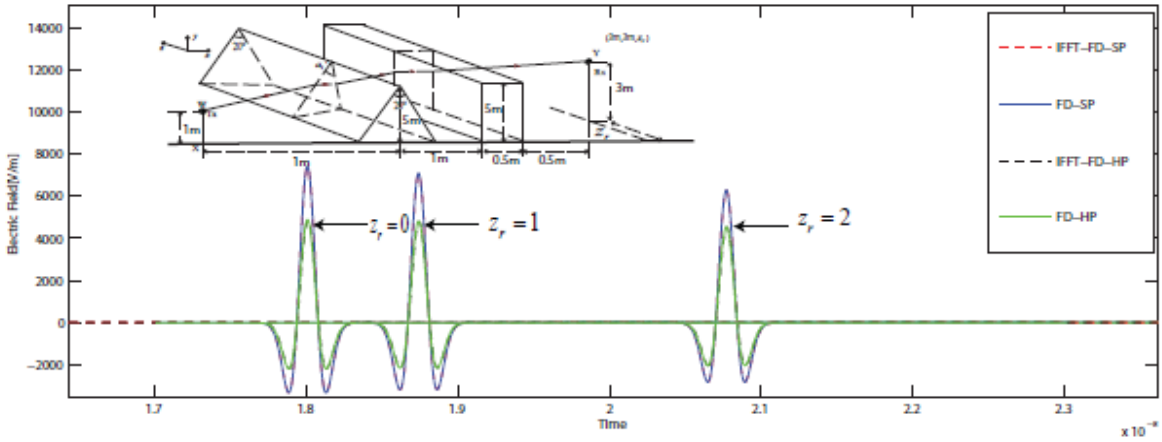

Figure 5.13: Transmitted field through 3-D 'dielectric wedge followed by a dielectric slab' for different receiver positions along z-axis with respect to transmitter, with glass.

A comparison between the computation times of the IFFT-FD method and the proposed TD solution for propagation profile considered in Fig. 4.1 & 4.2 is presented in Table 4. The presented results in Table 4 establish that the proposed TD analysis is computationally very efficient in comparison to the IFFT-FD solution.

Table 4: Efficiency comparison of two methods

Propagation profile	$T_{IFFT-FD}/T_{TD}$
For soft polarization	~198
For hard polarization	~191

The two main reasons for such a significant reduction in the computational time in TD are: (i) the efficient convolution technique [18] due to which few number of time samples suffice to provide accurate results. (ii) Approximation of the multiple transmission paths in FD by a single effective path for low-loss dielectric case.

Given the excellent agreement between proposed TD solution and IFFT of FD solution, it can be concluded that the proposed method is accurate for low loss tangent values in the UWB bandwidth. The presented work also establishes that the proposed TD solution is computationally more efficient than the conventional IFFT-FD method.

Chapter 6

FUTURE SCOPE/CONCLUSION OF WORK

In this work, different Time-domain heuristic coefficients are proposed based on the already established heuristic FD diffraction coefficients. The proposed heuristic coefficients are compared with the IFFT of the Rigorous solution to validate the results. Both the hard and soft polarizations have been considered. We have also produced a TD diffraction coefficient which is perfectly symmetrical & reciprocal for any arbitrary position of transmitter and receiver. With the TD formulation, the diffraction coefficients are more computationally efficient and distortion in the transmitted signal can be directly examined. An analytical TD solution has been presented for the transmitted field through 2-D & 3-D multi-modeled obstacles made up of low-loss dielectric materials. The results of the proposed TD solution are validated against the corresponding IFFT-FD results and the computational efficiency of two methods is compared. The TD solution outperforms the IFFT-FD analysis in terms of the computational efficiency. The TD solution is vital in the analysis of UWB communication as it can provide a fast and accurate prediction of the total transmitted and diffracted field in microcellular and indoor propagation scenarios.

The TD solution for the Maliuzhinets (RDC) solution can be produced for the prediction of diffracted field through a dielectric wedge for the future work.

References

1. Homayoun Nikookar, Ramjee Prasad,"*Introduction to Ultra Wideband Communication for Wireless Communication*" Springer ScienceþBusiness Media B.V. 2009
2. W. Stallings, *Wireless Communications and Networks*, Prentice-Hall, New Jersey, 2002, ISBN 0-13-040864-6.
3. C. A. Balanis, Advanced engineering electromagnetic. Wiley, New York, 1989.
4. Kazimierz Siwiak, Debra Mc. Keown, "*Ultra-Wideband Radio Technology*," John Wiley & Sons, Ltd, 2004. Chapter 2, pp. 30-31
5. J. B. Keller, "Geometrical Theory of Diffraction," *J. Opt. Soc. America*, vol. 52, 116-130, 1962.
6. R. G. Kouyoumjian, P. H. Pathak, "A Uniform Geometrical Theory of Diffraction for an Edge in a Perfectly Conducting Surface," *Proc. IEEE*, Vol. 62, 1448-1461, 1974.
7. R. J. Luebbers, "A Heuristic UTD Slope Diffraction Coefficient for Rough Lossy Wedges," *IEEE Trans. Antennas Propag.*, Vol. 37, 206-211, 1989.
8. P. D. Holm, A New Heuristic UTD Diffraction Coefficient for Nonperfectly Conducting Wedges," *IEEE Trans. Antennas Propag.*, Vol. 48, 1211-1219, 2000.
9. H. M. El-Sallabi, "A New Heuristic Diffraction Coefficient for Lossy Dielectric Wedges at Normal Incidence," *IEEE Antennas Wireless Propag. Lett.*, Vol. 1, 165-168, 2002.
10. Robert J. Fontana, "A Brief History of UWB Communications," Multispectral Solutions, Inc., Kluwer Academic/Plenum Publishers,2000.
11. R. J. Fontana, "Recent System Applications of Short-Pulse UWB Technology," *IEEE Trans on Microwave Theory and Techniques*, Vol. 52, No. 9, pp. 2087-2104, Sep. 2004.
12. P. Tewari, and S. Soni, "Time-domain solution for transmitted field through low-loss die-lectric obstacles in a microcellular and indoor scenario for UWB signals," IEEE Trans. Veh. Technol., 2013.
13. D. N. Schettino, F. J. S. Moreira, K. L. Boges, and C. G. Rego, "Novel heuristic UTD coefficients for the characterization of radio channels,"*IEEE Trans. Magnetics*, vol 43, no.4, pp. 1301-1304, April 2007.
14. M. Adi and J. Lavergnat, "Comparison of Luebbers' and Maliuzhinets' wedge diffraction coefficients in urban channel modeling," *Progress Electromagn. Res.*, pp. 1-28, PIER 33, 2001.
15. Maliuzhinets, G. D., Excitation, reflection and emission of surface waves from a wedge with given face impedances," *Sov. Phys. Doklady*, Vol. 3, 752-755, 1958.
16. Puspraj Singh Chauhan, and Sanjay Soni," A Novel Symmetrical Heuristic Coefficient for Urban Microcellular Environments" *International Journal of Information and Electronics Engineering, Vol. 2, No. 2, March 2012*
17. A. Karousos, C. Tzaras, "Multiple Time Domain Diffraction for UWB Signals," *IEEE Trans. Antennas Propag.*, Vol. 56, 1420-1427, 2008.

18. E. O. Brigham, *Fast Fourier transform and its applications*, Prentice Hall, 1988.
19. M. Ghavami, L. B. Michael, and R. Kohno, *Ultra Wideband Signals and Systems in Communication Engineering*. Chichester, U.K.: Wiley, 2004.
20. D. Porcino, and W. Hirt, "Ultra-Wideband Radio Technology: Potential and Challenges Ahead," *IEEE Communications Magazine*, 66-74, 2003.
21. R. C. Qiu, C. Zhou, and Q. Liu, "Physics-Based Pulse Distortion for Ultra-Wideband Signals," *IEEE Trans. Vehicular Technology*, vol. 54, 1546-1555, 2005.
22. P. Liu, J. Guo, J. Liu, J. Wang, and Y. Long, "Multiple Time-Domain Diffraction of Plane Waves by an Array of Perfectly Conducting Wedges for UWB signals," *978-1-4244-5708-3/10 2010 IEEE*, 1173-1176, 2010.
23. T. W. Veruttipong, "Time-Domain Version of the Uniform GTD," *IEEE.Trans. Antennas Propag.*," vol. 38, 1757–1764, 1990.
24. P. Rousseau and P. Pathak, "Time-Domain Uniform Geometrical Theory of Diffraction for a Curved Wedge," *IEEE Trans. Antennas Propag.*," Vol. 43, 1375–1382, 1995.
25. P. Górniak and W. Banduriski, "Direct Time-Domain Analysis of an UWB Pulse Distortion by Convex Objects with the Slope Diffraction Included," *IEEE Trans. Antennas Propag.*, vol. 56, 3036–3044, 2008.
26. P. R. Rousseau and P. H. Pathak, "A Time-Domain Formulation of the Uniform Geometrical Theory of Diffraction for Scattering from a Smooth Convex Surface," *IEEE Trans. Antennas Propag.*, vol. 55, 1522–1534, 2007.
27. A. Karousos and C. Tzaras, "Time-Domain Diffraction for a Double Wedge Obstruction," *in Proc. IEEE AP-S Int. Symp.*," Honolulu, HI, 4581–4584, 2007.
28. P. Liu and Y. Long, "Time-Domain UTD-PO Solution for Multiple Building Diffraction for UWB Signals," *Electronics Letters*, Vol. 45, 924-926, 2009.
29. T. Han and Y. Long, "Time-Domain UTD-PO Analysis of a UWB Pulse Distortion by Multiple Building Diffraction," *IEEE Antennas and Wireless Propagation Letters*, Vol. 9, 795-798, 2010.
30. P. Liu, J. Tan, and Y. Long, "Time-Domain UTD-PO Solution for the Multiple Diffractions of Spherical Waves for UWB Signals," *IEEE Trans. Antennas and Propagation*, vol. 59, 1420-1424, 2011.
31. Y. L. C. de Jong, M. H. J. L. Koelen, and M. H. A. J. Herben, "A Building-Transmission Model for Improved Propagation Prediction in Urban Microcells," *IEEE Trans. Vehicular Technology*, vol. 53, 490-502, 2004.
32. Z. Chen, R. Yao, and Z. Guo, "The Characteristics of UWB Signal Transmitting through a Lossy Dielectric Slab," *IEEE 60th Veh. Technol.Conf. (VTC2004-Fall)*, vol. 1, 134–138, 2004.
33. R. Yao, Z. Chen, and Z. Guo, "An Efficient Multipath Channel Model for UWB Home Networking," *0-7803-8451-2/04, IEEE*, 511-516, 2004.

34. R. C. Qiu, "A Generalized Time Domain Multipath Channel and Its Application in Ultra-Wideband (UWB) Wireless Optimal Receiver Design—Part II: Physics-Based System Analysis," *IEEE Trans. on Wireless Communications*, Vol. 3, 2312-2324, 2004.
35. Paul R. Barnes,"On the Direct Calculation of a Transient Plane Wave Reflected from a Finitely Conducting Half Space," IEEE transactions on electromagnetic compatibility, vol. 33, no. 2, may 1991
36. A. Muqaibel, A. Safaai-Jazi, A. Bayram, A.M. Attiya and S.M. Riad, "Ultra wideband through-the-Wall Propagation," *IEE Proc.-Microw. Antennas Propag.*, Vol. 152, 581-588, 2005.
37. W. Yang, Z. Qinyu, Z. Naitong, C. Peipei, "Transmission Characteristics of Ultra-Wide Band Impulse Signals," *Wireless Communications, Networking and Mobile Computing, 2007. WiCom 2007. International Conference*, 550-553, 2007.
38. W. Yang, Z. Naitong, Z. Qinyu, and Z. Zhongzhao, "Simplified Calculation of UWB Signal Transmitting through a Finitely Conducting Slab," *Journal of Systems Engineering and Electronics*, Vol. 19, 1070–1075, 2008.
39. A. Karousos, G. Koutitas, C. Tzaras, "Transmission and Reflection Coefficients in Time-Domain for a Dielectric Slab for UWB Signals," *Vehicular Technology Conference, 2008. VTC Spring 2008. IEEE*, 455-458, 2008.
40. S. Soni, A, Bhattacharya, "An Analytical Characterization of Transmission through a Building for Deterministic Propagation Modeling," *Microwave and Optical Technology Letters*, Vol. 53, 1875-1879, 2011.
41. Kate A. Remley, Harry R. Anderson, and Andreas Weisshar, "Improving the Accuracy of Ray-Tracing Techniques for Indoor Propagation Modeling," *IEEE Transactions on Vehicular Technology*, Vol. 49, No. 6, Nov.2000.
42. S. Soni and A. Bhattacharya," New heuristic diffraction coefficient for modeling of wireless channel," *Progress In Electromagnetics Research C, Vol. 12, 125-137, 2010*